Development and Evaluation of a Sand Pluviator

An Approach to Standardized Sample Preparation for Physical Modelling in Geotechnics

door

Yifan Yang

ter verkrijging van de graad van Master of Science
aan de Technische Universiteit Delft,
in het openbaar de verdedigen op vrijdag 20 november 2020 te 15:00 uur.

Student number:	4817508	
Project duration:	March 31, 2020 – November 20, 2020	
Thesis committee:	Dr. A. Askarinejad,	TU Delft, chairman
	Prof. dr. K. G. Gavin,	TU Delft
	Dr. F. Pisanò,	TU Delft
	Ir. D. A. de Lange,	Deltares | TU Delft
	Dr. H. Wang,	TU Delft

An electronic version of this thesis is available at `http://repository.tudelft.nl/`.

TUDelft

Preface

As it was said by Heraclitus that "No man ever steps in the same river twice", should I say that "No man ever does the same experiment twice"?

I have never attached such great importance to the standardization of sample preparation work for physical modelling before the meeting with Amin one year ago, and therefore, firstly, I would like to address my sincere thanks to him, the man who supervised me prudently and always encouraged me heading up for expensive experiments. Undoubtedly, it is Amin who made me have a brand new view of our magic field of geo-engineering.

I wish to express my gratitude to Dirk, with whom I discussed everything about the thesis. Indeed, he provided great advice and delicate polish to my thesis. I still remember the afternoons when we sat together at Deltares, and I am sure that would become my great mémoire. Deep thanks to Huan, it is my great honour to be guided by this genius man and his ideas rescued my project for many times. Many thanks to Ken, the professor from my thesis committee, who gave me advice, especially on the CPT tests. The online talk after the oral exam of his course was unforgettable, and after which, my targets of thesis work became remarkably clear. My gratitude is also directed to Federico, another expert from the committee. His advice on the fabric study of sand was so helpful that I spent more than half of desk working time on the papers from Grenoble and Saitama, and that would be a brand new world for me. I would like also to address my special thanks to Wout, the designer of our sand pluviator. His smile is always encouraging, and his design is undoubtedly great, providing me with the precious opportunity working on this thesis topic.

I appreciate the support from Paul, who did a lot of maintenance work for this delicate pluviator. The days when we worked together were so glamorous. I am also very grateful to Kees, Karel, Roland, Marc, Jens, Wim, Joost, Ellen, Han and Ton, the technical support staff from DEMO, GSE lab and Stevin II lab of TU Delft. Without their help, the thesis work that I am feeling proud of would not exist at all.

I cherish the days working with Yuen, he helped me so much and I will never forget his handsome figure in the pilot seat of our centrifuge. The days working with Xuehui were exciting as well, for months we met almost every day and we have done great teamwork in Delft, Mol and Barendrecht. During my dilemma of selecting undisturbed sampling approaches, Aoxi provided me with much guidance on the bio-cementation methods, deep thanks to him. Weiyuan, our charming expert of geo-centrifuge, helped me from selecting the thesis topic to the final stage of shallow foundation experiment, deep thanks to him. The sweet bro Haoyuan gave me a lot of suggestions from the literature review work until the typesetting of bibliography, and I am so grateful. Xiangcou generously encouraged me re-sorting the tests during the most difficult summer time, thanks a lot. Special thanks to Kevin, who helped me with the English language for technical writing. I appreciate the help from Bun san, with the literature, which was very crucial to my project. Also, many thanks to Jiang san, the expert of DEM, who advised me from the beginning of the thesis work. As my topic is totally outside the field of continuum mechanics, his professional views on discrete granular materials benefited me greatly.

Lastly, I would like to thank my parents for their unconditional support, and thank my friends with whom we shared laughter and tears together in Delfgauw.

Many thanks again to everyone, we experienced the tough coronavirus crisis together, and we are looking forward to the wonderful future, cheers.

Yifan Yang
Röntgenweg, Delft, November 2020

Abstract

For preparing standardized sand specimens for physical modelling in geotechnics, especially for the geo-centrifuge tests, a "line-style" sand pluviator has been recently developed by TU Delft. Controlling the falling height of sand hopper, the width of hopper's bottom gap and the relative moving speed between the hopper and the sample box, specimens with bulk relative density ranging from 50% to 100% can be prepared by this automated machine using the coarse Merwede River sand. Besides, the periodic variation of local relative density along depth was observed using the macro-CT scanner and the features of the fabrics were investigated using the micro-CT scanner. It was also proved by a set of shallow foundation modelling tests that the sand specimens having the same bulk relative density but different heterogeneity and fabric features behaved significantly differently and further research works are recommended to explore the influences of these differences. Additionally, a partially substantiated hypothesis was proposed to conclude the general rules of the sand pluviation process, and the reliability of this hypothesis has been proved by a series of tests on the Geba sand.

Contents

1

Introduction

1.1. Background

Physical modelling in geotechnics includes in particular small-scale tests to simulate prototype geotechnical problems and requires prudent preparation work for test models, as any subtle alteration of pre-designed physical modelling parameters (e.g. the relative density for sand specimens) would result in deviation in the test results (see e.g. Schofield, 1980; Madabhushi et al., 2006), which could be unacceptable. Therefore, for physical modelling in geotechnics, it is necessary to standardize the sample preparation process, to make the samples have precisely controllable parameters, especially for repetitive tests.

For standardized preparation work for sand specimens, controlling the features of particles (e.g. density, roughness and roundness) and fabrics (e.g. compactness, alignment and contact of particles) are crucial, as these features are basically all the potential variables for the sand packing itself. For a certain type of industrial sand product, the features of particles could be considered as constant and therefore, the changeable features of fabrics become the only challenges of standardization.

As mentioned above, the fabric features of a certain type of sand can be described in various aspects, and making all of them precisely controllable is undoubtedly difficult. During the past decades, it was found that one of the fabric features, the compactness of particles has exceptionally significant effects on the behaviour of sands (see e.g. Lee, 1965; Bolton, 1986). Besides, the compactness of a certain type of sand can be easily quantified by the index Relative Density (D_r). Therefore, scholars were taking priority researching methods controlling the relative density of sand samples for the standardization of their preparation work.

Consequently, a series of reconstitution methods have been proposed, including the shovelling, tamping and vibrating methods by which the porosity of sand is adjusted after deposition and in terms of these methods, strongly anisotropic properties (Butterfield and Andrawes, 1970) and significantly vertical inclination of sand particles (Arulanandan, 1978) are noticeable. On the other hand, another method named the pluviation method, by which the porosity is adjusted during deposition, by controlling the height of fall of the sand grains and the rate of deposition was proposed (Kolbuszewski, 1948), developed (see e.g. Kolbuszewski and Jones, 1961), and automated (see e.g. Garnier and Cottineau, 1988), and the machines were generally named as the sand pluviators.

Although the relative density is not the only index for describing various aspects of fabric features of sand, it is still of significance to make the relative density controllable using a proper reconstitution method, and the sand pluviation method could be a good approach.

1.2. Research Objectives and Methods

To explore the pluviation method's potential contribution to the standardization of sample preparation work, first of all, a sand pluviator should be designed, manufactured, and calibrated. Then, using a specific type of sand (the coarse Merwede River sand), a series of pluviation tests should be done to explore the performance of the sand pluviator on controlling the (bulk) relative density of sand specimens, as it is the original intention of developing this machine. Afterwards, the homogeneity of pluviated sand specimens should be checked, as they are not impossible to be significantly heterogeneous. Next, based on the research mentioned above, general rules of the sand pluviator's influences on the relative density and its homogeneity of sand specimens,
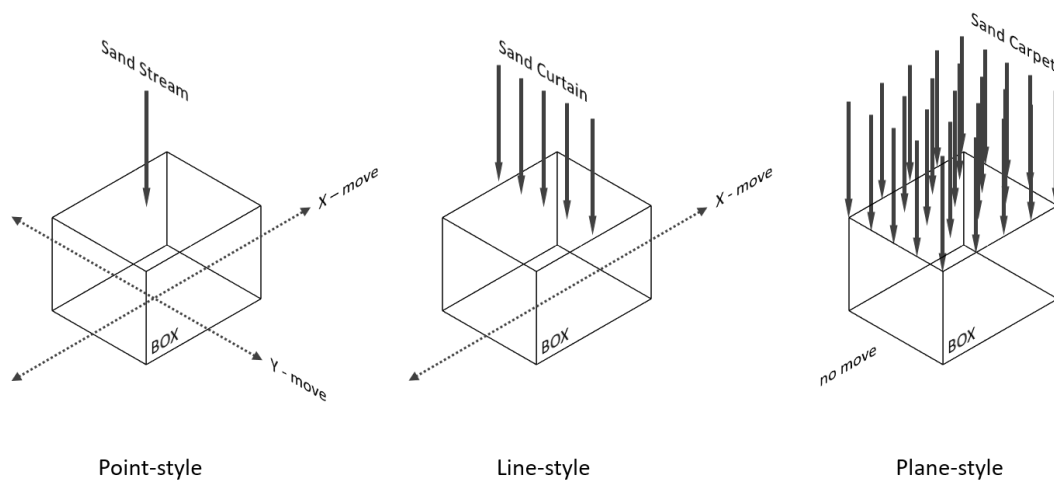
Figure 1.1: Point-, line- and plane-style sand pluviation concepts

including the mechanisms of the sand pluviation process should be concluded. These general rules should be examined by tests on a new type of sand (the Geba sand).

In addition to focusing on the prioritized index of sand particle packing's compactness (i.e. the relative density), other fabric features of pluviated sand specimens should be observed as well. Several indexes should be used to quantify and then evaluate these features.

Lastly, the behaviour of pluviated sand specimens in physical modelling tests should be discussed. It has to be acknowledged that the behaviour of sand specimens is a grand topic of various aspects, including drained/undrained, large strain/small strain, monotonic/cyclic, mechanical/hydro-mechanical, etc., and hence, it is infeasible to discuss many of them in this study. Therefore thus, here is no specific literature review for the behaviour of pluviated sand specimens in this section, and the selected and detailed discussions are introduced in Section 3.7.

1.2.1. Developing a Sand Pluviator

The basic concept of the sand pluviation method is to pour sand grains into the sample boxes from a certain height. To make the falling particles form a relatively steady and continuous stream, the sand grains should usually go through a container which has an aperture or a set of sieves at the bottom. The sand pluviators are generally divided into three types. For the first type, sand grains go through a hole whose scale is significantly smaller than that of sample box and hence, to fill the box, the relatively horizontal movement between sand stream and sample box in both X- and Y- direction is indispensable. This type of sand pluviators are called the "point-style" ones (see e.g. Hakhamaneshi et al., 2016). For the second type, the opening gap located at the bottom of the sand container has a shape of long strip and by going through which, the sand particles form a curtain-shaped flow and the the relatively horizontal movement between the "sand curtain" and the sample box is needed in only one direction (i.e. the direction which is perpendicular to the "sand curtain"). This type of sand pluviators are called the "line-style" ones (see e.g. Stuit, 1995). For the third type, the bottom of the sand container is usually a sieve or a set of sieves and the area of which is larger than that of sample boxes. Therefore, the falling particles form a "sand carpet" at a certain moment and no relatively horizontal movement between the sand container and the sample box is needed. This type of sand pluviators are called the "plane-style" ones (see e.g. Choi et al., 2010). The concepts of these three types of sand pluviators are shown in Figure 1.1.

During the past decades, various sand pluviators were developed by numerous institutions worldwide (see e.g. Garnier and Cottineau, 1988; Lo Presti et al., 1993; Fretti et al., 1995; Madabhushi et al., 2006; Lagioia et al., 2006; Choi et al., 2010; Dave and Dasaka, 2012; Khari et al., 2014; Hakhamaneshi et al., 2016; Hariprasad et al., 2016; Hossain and Ansary, 2018). And it was stated that the relative density of sand samples are generally able to be controlled using the sand pluviation method. As the sand pluviation method has been recommended by many research works, at TU Delft, a new sand pluviator was developed as well. Although the (dis)advantages of the three types of sand pluviators cannot be concluded comprehensively based on literature review, following the domestic pioneer research (i.e. Stuit, 1995), the "line-style" was selected, and

the design of the TU Delft sand pluviator is introduced in Chapter 2.

1.2.2. The Relative Density of Pluviated Sand Specimens

It was initially indicated by Kolbuszewski (1948) that the falling height and the rate of deposition are the key variables of the ultimate relative density of pluviated sand specimens. Besides, as mentioned above, for the sand pluviation process, the horizontally relative movement between the sample box and the (vertically) falling sand particles is necessary, except for the rare plane-style pluviator, and it was revealed that the relative moving speed has effects on the relative density as well (see e.g. Stuit, 1995; Bolouri Bazaz et al., 2018).

Therefore, these three variables' influences on the specimens' relative density should be explored by a series of pluviation tests and the detailed optical observation by high frame rate (HFR) camera shooting. A Canon EOS 750D digital camera was used in this work, and the maximum frame rate of this camera is 50 frames per second.

Additionally, the pluviation test results (i.e. the "recipes" of variables for specimens of certain values of relative density) for certain types of sands could be considered as pre-calibration for future sample preparation work.

1.2.3. The Homogeneity of Pluviated Sand Specimens

It has been indicated by many scholars that the sand samples prepared by the pluviation method are not always ideally homogeneous, according to their results of cone penetration tests (see e.g. Corté et al., 1991; Fretti et al., 1995), lamel ring container tests (Stuit, 1995) and mold tests (see e.g. Choi et al., 2010). For example, according to the cone penetration tests performed at 1g in dry pluviated Fontainebleau sand (Corté et al., 1991), the value of the cone resistance varied obviously in the vertical direction with a certain frequency, which indicated the existence of distinct denser and looser sand layers in the pluviated specimens. As the homogeneity checking methods mentioned above (e.g. cone penetration tests) may disturb the fabrics of sand specimens and thence, the computed tomography (CT) method, the one based on the penetration results of X-ray beams which do not disturb the sand particles mechanically, is recommended for this research. As well known, by recording of sets of attenuation profiles of collimated X-ray beams through a body in different directions in a plane and subsequently solving the system of linear equations, the distribution of local radiographic density in a certain plane can be achieved. The electromagnetic radiation related tomography methods have been successfully applied in soil mechanics for decades and it has been proved that the calculated radiographic density basically has a positive linear correlation with the density of sand packing (see e.g. Desrues et al., 1996). For a certain type of sand, as the particle density, maximum and minimum void ratio can be considered as constant and hence, the calculated radiographic density of CT can be considered as having a positive linear correlation with the relative density. Although this back-calculating work based on local radiographic density is only a qualitative method, rather than a quantitative one for figuring out the local relative density of sand packing when without sophisticated pre-calibration work, the CT is still capable of distinguishing the local D_r's variance of different extents, even for different specimens, as long as the bulk D_r is calculated using the conventional method (i.e. measuring the volume and mass of sand packing directly). Therefore, the mature and reliable computed tomography method was chosen and a Siemens Somatom medical CT scanner of TU Delft (referred to as the macro-CT) was used in this work. A photo of the macro-CT is shown in Figure 1.2.

1.2.4. Other Fabric features of Pluviated Sand Specimens

As explained before, controlling the relative density is not the only mission for the standardization of sand samples' preparation work. For a certain type of natural silica sand, the fabric features (e.g. the inclination of grains' longest axes) of different specimens could vary, even for those with the same void ratio. The specimens prepared by different methods could have different fabric features (Arulanandan, 1978) and the dissimilar fabrics usually result in the differences in sands' mechanical behaviour (see e.g. Oda, 1972a, 1972b; Oda and Koishikawa, 1978; Miura and Toki, 1982; Bowman and Soga, 2003). Therefore, for evaluating specimens prepared by the sand pluviation method, studying the fabric features is indispensable.

The Phoenix-Xray CT scanner of TU Delft (referred to as the micro-CT) was planned to be used to observe the fabrics of prepared sand samples, as the previously used macro-CT scanner has the finest resolution of 0.3 mm, and with which, the shapes of sand particles (grain size < 2mm, typically < 1 mm) are obviously impossible to be depicted. The micro-CT scanner has the resolution of up to 0.5 μm and it has been proved by a set of pre-tests that it is possible to reconstruct the tomographic shapes of the coarse Merwede River sand particles (D_{50} 0.73 mm). A photo of a sample box being scanned by the micro-CT is shown in Figure 1.3.
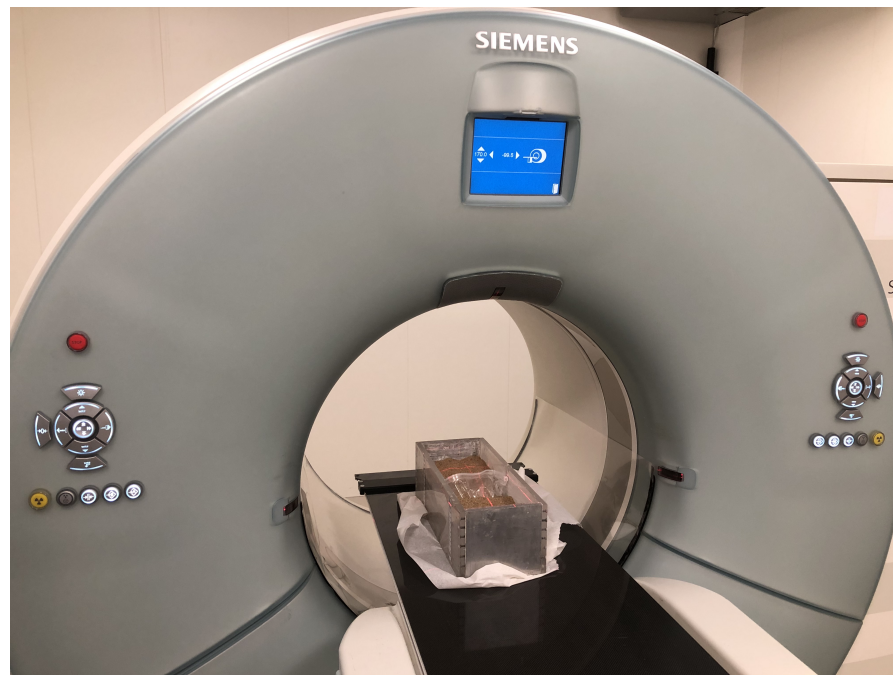
Figure 1.2: The macro-CT of TU Delft

However, it is a challenge that for the micro-CT scanner, the maximum diameter of tested samples is 12 cm and this size is significantly smaller than that of regularly used sample boxes. What is more, the resolution of reconstructed CT images is higher when a smaller sample is scanned and thus it is empirically recommended that the sand sample to be scanned has an axial length of maximum 8 cm and a radial diameter of maximum 4 cm. Therefore, it is necessary to take small and undisturbed packing of sand from the prepared specimens.

Three methods were proposed to solve this problem. The first one is to saturate dry specimens with polyester resin and then cut the hardened specimen by a diamond saw into small pieces, as what Oda (1972a, 1972b) has done. However, the resin material is toxic but no special protective and ventilation equipment was available in the laboratory and therefore, this plan was abandoned. The second plan is to cement the sand specimens by the bio-cementation methods such as the microbial induced carbonate precipitation (MICP) method (see e.g. Gomez et al., 2018) or the microbial induced desaturation and precipitation (MIDP) method (see e.g. O'Donnell et al., 2017). However, as the bio-cementation methods have not been applied widely and are still in need of further research, this plan was abandoned as well. The third plan is to saturate a pluviated sand specimen with water and then freeze the whole saturated specimen (with the box) at -24°C. When the whole specimen is frozen, a diamond drill should be used to take a cylindrical sample out, and the diameter of the diamond drill was chosen to be 3 cm.

As the micro-CT scanning process usually lasts more than 60 minutes, the frozen sand sample may melt significantly during this long time period, even when being protected by a pre-cooled adiabatic case made of foam. The melting process results in the intolerable movement of sand particles and then make the quality of reconstructed CT images bad. Therefore, the frozen samples must be processed physically before being scanned by CT, and the processing method is sketched in Figure 1.4. Firstly, a cylinder container made by polyvinyl chloride (PVC) is prepared and the diameter of the container should be larger than that of the drilled frozen sample. It should be mentioned that the container has some holes at the bottom to make free drainage possible. Some finer sand (finer than the frozen sand, and in this case, D_{50} of the finer sand is 0.35 mm) is then put into the container to cover the bottom, as shown in Figure 1.4a. After that, the frozen sample is carefully put into the container and one should pour more fine sand into the container to surround the frozen sample. Meanwhile, the container should be vibrated gently to make the surrounding sand dense. When the frozen sample is fully surrounded by fine sand, the whole container can be left in the room temperature and thence the frozen sample will melt and the water will drain via the holes at the container's bottom, as shown in Figure 1.4b, 1.4c and 1.4d. After more than one day, no ice exists in the cylindrical sample and then the sample, especially the part of interested marked in the dashed frame, can be scanned by the micro-CT for a
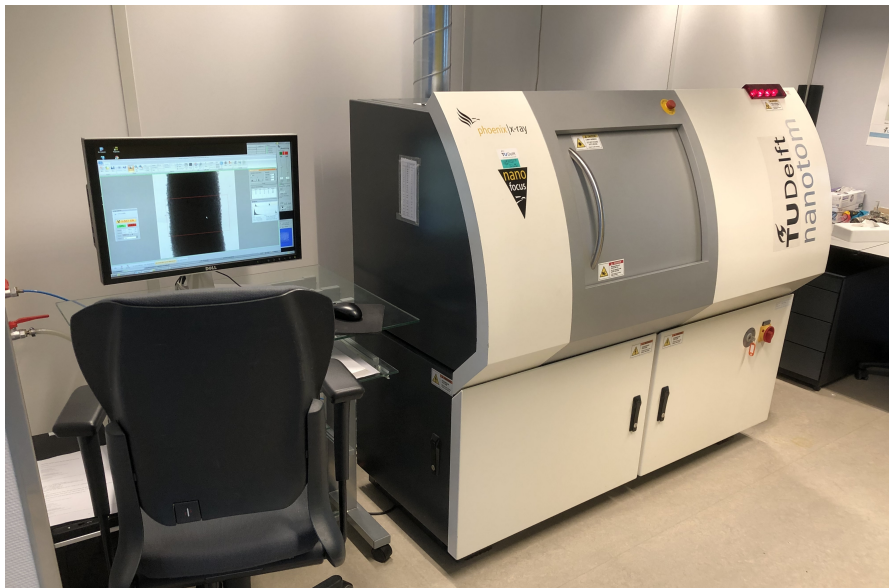
Figure 1.3: The micro-CT of TU Delft

long time period, as shown in Figure 1.4e.

It must be noticed that during the process of freezing, the volume of water may increase by approximately 10% and it is possible that the sand particles are disturbed by the frozen water. Although it has been proved by Oda (1972a) that particles of the frozen-and-melted samples are disturbed very limitedly (e.g. axial strain of less than 1%), exploring the influence of freezing is still of importance and thus a set of pre-tests were done. According to the trials, it was observed that there always forms one or several "icebergs" in the saturated sample box, when being frozen and the upheaval is more obvious in the area near the "iceberg(s)". What is more, it was subsequently found that the upheaval of sand particles becomes more insignificant when the water level is much (e.g. 50%) higher than the height of sand layers, as the "iceberg" always floats in water. Based on these two conclusions, it is required that the level of saturating water must be high and the "iceberg(s)" must be kept far away from the area of interest as much as possible.

Therefore, a pair of foam cases were designed empirically and these cases tightly cover the sample box, insulating the covered part from the atmosphere of low temperature, as shown in Figure 1.5. By using the foam cases, the whole saturated sample must be kept in the freezer of -24°C for at least 4 days before its thoroughly being frozen and in comparison, a similar saturated sample can be frozen within 10 hours when it is not covered by the foam cases. With a high water level and a special pair of adiabatic cases, the upheaval of ice should concentrate on the two sides of the sample box and the upheaval in the middle is relatively negligible, the undisturbed area is shown in the dash frame of Figure 1.6.

A series of photos were taken by a camera with a fixed tripod to observe the movements of sand particles before- and after- the freezing process. It was found that the relative displacement and rotation of particles in the area of interest (dash frame of Figure 1.6) cannot even be detected by processing photos with a high resolution of 6000 × 4000 pixels and thence, the sand sample can be considered as undisturbed during the process of freezing, when using the special "tricks" mentioned above.

drilled frozen sample of coarse Merwede River sand   fine Merwede River sand

melting and drainage

a   b   c   d   e
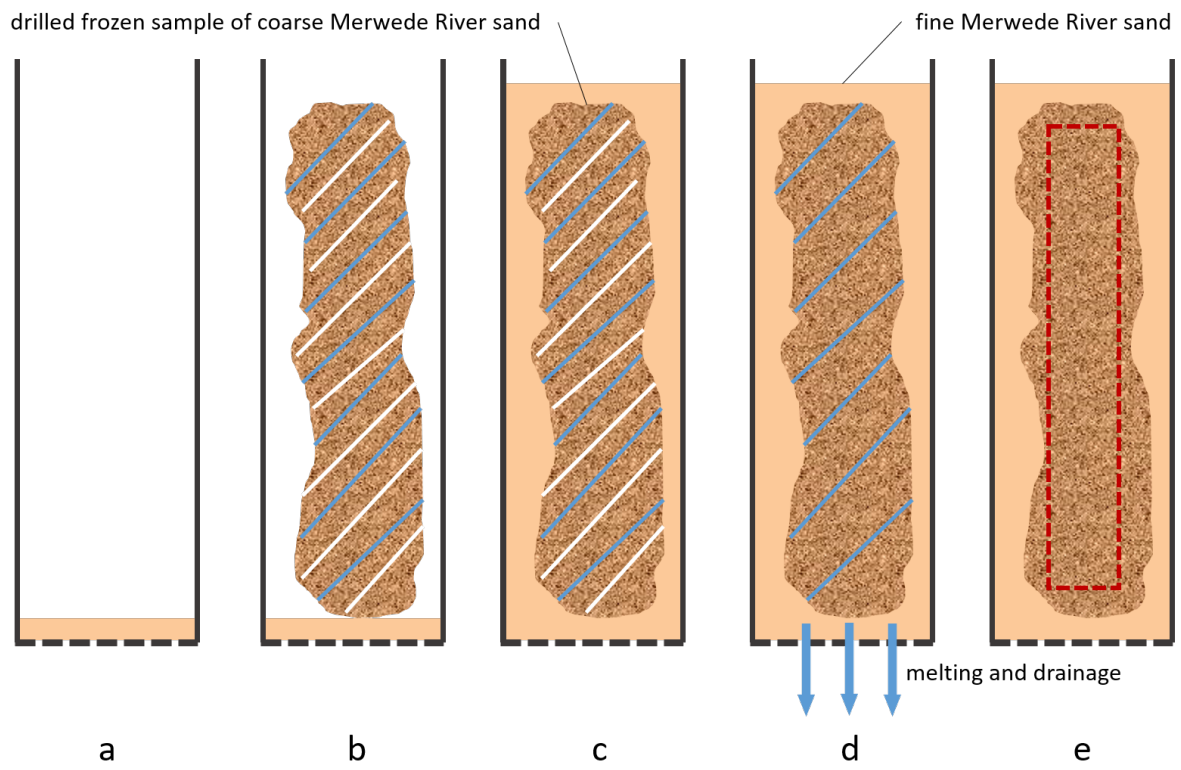
Figure 1.4: Processing method for undisturbed sampling for micro-CT scanning

Figure 1.5: The frozen saturated specimen with controllable upheaval by using foam covers
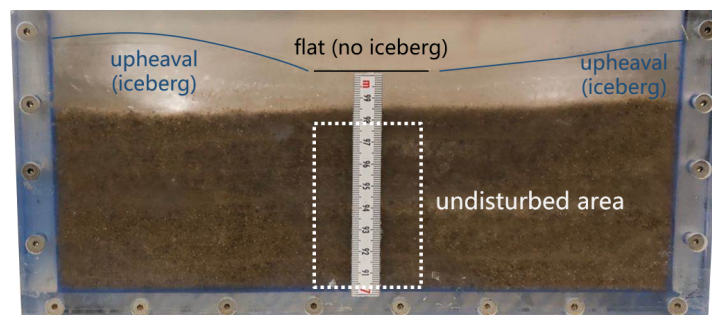
upheaval
(iceberg)   flat (no iceberg)   upheaval
(iceberg)

undisturbed area

Figure 1.6: The frozen saturated specimen with controllable upheaval by using foam covers

2

The TU Delft Sand Pluviator

2.1. General Description

As mentioned in Chapter 1, the TU Delft sand pluviator is an automatic "line-style" pluviator, and it was developed in 2016, referring to the designing concept of the old TU Delft sand pluviator (Stuit, 1995). As shown in Figure 2.1, the device has a triangular-prism shaped sand hopper which contains the sand temporarily. A slot located at the bottom ridge of the sand hopper can be opened manually and the opening width can be adjusted by a spiral caliper. By screwing the spiral caliper, changing the gap width, the thickness of the "sand curtain", which is positively correlated with the sand grains' raining intensity (Lo Presti et al., 1993; Bolouri Bazaz et al., 2018) can be controlled. Meanwhile, the height of sand hopper can be adjusted by driving two vertical transmission belts.

The sand grains which were previously stored in the closed hopper can fall down freely via the line-shaped gap (slot) and hence a "sand curtain" forms. Then, driven by two horizontal transmission belts, with a controllable speed, the sample box starts moving from the starting point (i.e. the most right-hand side of the horizontal transmission belt, as shown in Figure 2.1), going through the "sand curtain" and thus a layer of sand grains can be deposited in the box. Next, the box continues moving forward (towards the left-hand side of the horizontal transmission belt, as shown in Figure 2.1) until arriving at the ending point below the laser rangefinder, where the pre-calibrated rangefinder can be used to measure the height of accumulated sand layers. Afterwards, the box should move back to the starting point and the hopper with depleted sand should be refilled for the next deposition loop. With the deposition loop continues, sand grains accumulate in the sample box layer by layer, until the target height of sand body is reached.

It is noticeable that not all the sand grains can be deposited in the sample box and those which fall outside the box are held and then transported to a cubic sand container, by a wide recycle belt located beneath those belts which drive the sand box. Sand grains accumulating in the cubic recycle container can be transported upwards to refill the sand hopper, by an electric vacuum pump. The power of the vacuum pump is 8000 watts and this pump is capable of transporting approximately 20 kilograms of sand in 3 minutes, via a plastic tube protected by a metal pipe and the inner diameter of plastic tube is 5 centimetres. Additionally, assistant shovelling work is needed to transport the sand stored in the recycle container towards the plastic tube.

According to the researches on the similar "line-style" sand pluviators by Stuit (1995) and Bolouri Bazaz et al. (2018), three execution parameters were selected to be the variables to control the relative density of pluviated sand samples, and these variables are: the width of the opening gap at the bottom of the sand hopper, referred to as the Opening Width; the falling height of sand grains, measured from the bottom free surface of the sand stored in the hopper to the sand surface which the falling grains finally hit, referred to as the Falling Height; and the horizontal moving speed of the sample box when going through the "sand curtain", referred to as the Box Speed.

The accuracy, maximum and minimum values of the three variables and their controlling methods are shown in Table 2.1.

---

[1]The minimum Falling Height should be determined by the height of sample boxes. As the width of frequently used sample boxes are smaller than that of the sand hopper and therefore, the sand hopper should always be above the sample boxes. For instance, if the height of a sample box is 15 cm, the minimum value of the Falling Height should be set as no less than 15 cm to avoid potential collisions or scratches between the sand hopper and the sample box.

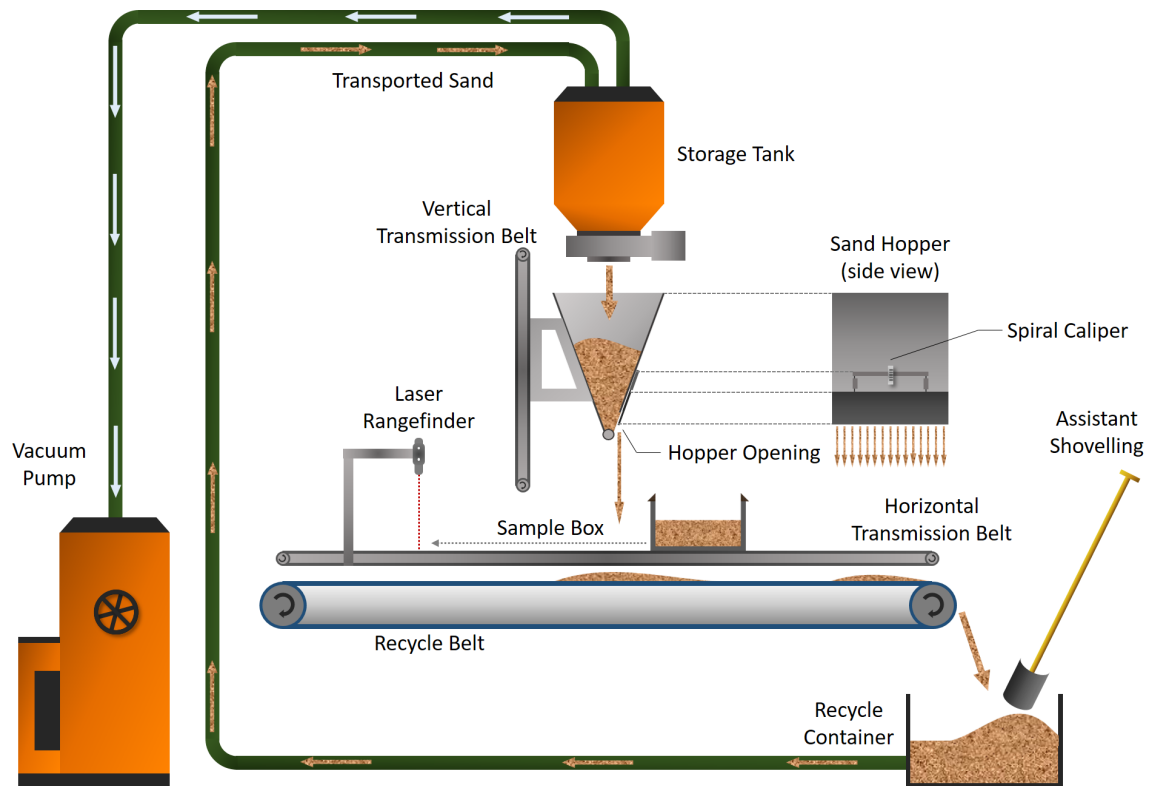Figure 2.1: Sketch of the TU Delft sand pluviator

Table 2.1: Variables of the TU Delft sand pluviator

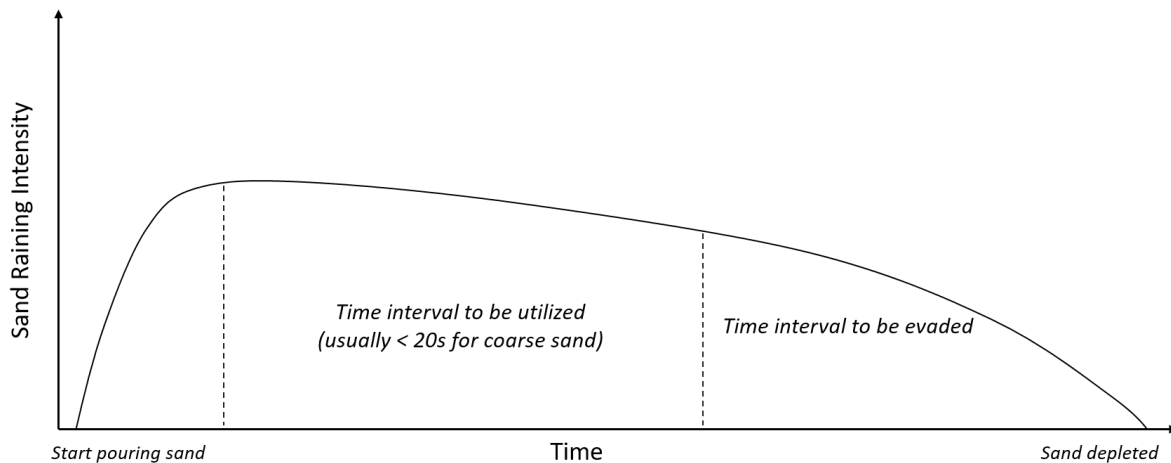| Variable	Controlling method	Max. value	Min. value	Accuracy
Falling Height	Servo motor belt (vertical)	1080 mm	t.b.d.[1]	1 mm
Opening Width	Spiral caliper	25 mm	0	1 μm
Box Speed	Servo motor belt (horizontal)	90 mm/s	0	1 mm/s

Figure 2.2: Sand raining intensity along time (a rough estimation)

2.2. Challenges

It is worthy of mentioning that the three variables are not all the factors affecting the relative density of samples made from a certain type of sand. The fullness of sand hopper, the flatness and the initial relative density of sand stored in the hopper, dust and moisture in the sand do influence the sample preparation work significantly and these indexes become the challenges for the TU Delft sand pluviator to prepare standardized sand specimens.

The first challenge is the fullness of the sand hopper, which affects the sand raining intensity directly and has been proved to have an influence upon the ultimate relative density of the prepared specimens (see e.g. Hakhamaneshi et al., 2016). For a hopper which is never refilled with sand before depletion, according to the rough estimation based on the ruler stuck inside the hopper, the general relationship between time and sand raining intensity is shown in Figure 2.2. As can be seen from the curve, when opening the bottom gap, the sand grains start falling down and the raining intensity increases sharply from zero. After reaching the peak at an initial stage, the value of the raining intensity starts decreasing slowly. At the final stage, the sand grains remaining in the hopper become very few and thence the raining intensity decreases significantly, and the "sand curtain" will eventually disappear when the stored sand is completely depleted.

Obviously, only the middle time interval can be utilized and the final stage must be evaded, otherwise the relative density of the ultimately prepared specimen would be much larger than expected. For example, when using the coarse Merwede River sand (D_{50} 0.73 mm) and setting the Opening Width as 3 mm, the Box Speed as 1.5 mm/s, the time of relatively stable raining intensity (the middle stage in Figure 3) is approximate 20 seconds, which allows the sample box to go through the "sand curtain" for twice. In this occasion, if one sets the Falling Height as 28 cm, the relative density of the prepared sample should be about 80%. However, if one does not stop the pluviation process to refill the sand hopper and let the sample box go through the "sand curtain" for a third and a fourth time, the relative density may increase to approximately 90% as a result. Therefore, before starting the formal pluviation process, one must observe the depletion of the sand stored in the hopper and estimate the "good" time interval when the sand raining intensity is relatively stable.

Because of the low efficiency of the sand's being recycled by the vacuum pump, the speed of refilling sand is significantly lower than sand's losing from the hopper and the hopper can only be refilled slowly when the pluviation process is paused. Therefore, an absolutely unchanged fullness of sand is impossible and that makes the fullness the first challenge for preparing standardized sand specimens by the TU Delft sand pluviator.

The second challenge is the initial state (e.g. flatness and relative density) of sand stored in the hopper. As shown in Figure 2.1, the opening aperture of the orange container for refilling sand is significantly smaller than the hopper and thence the refilled sand will naturally form a dune in the hopper, as shown in Figure 2.3a. According to the observation, when the sand body in the hopper is not flat, the raining intensity along the strip-shaped opening gap will not be uniform. In other words, the "sand rain" is relatively heavy right beneath the sand dune and but relatively light on the two sides. Therefore, it is necessary to make the sand flat every time when the refilling process is finished. Since the vibratory action (e.g. hammering the sand hopper) was

(a) before shovelling

(b) after shovelling

Figure 2.3: Flatness comparison of sand stored in the hopper

not observed as effective to make the stored sand dune flat, a tiny shovel can be used, as shown in Figure 2.3b. Although the criterion for "flatness" is not strict, it is empirically recommended by the author that one should keep shovelling the surface of sand until there is no slopes whose inclination is larger than 10°.

Meanwhile, the initial relative density of sand before pluviation is important as well, although there were no comparison tests specially designed to check the influence of that index. It is recommended by the author that for each time refilling the hopper, one should set the hopper at an unchanged height (e.g. the highest position). Besides, after the refilling process is done, the sand dune must be shovelled (to be flat) as gently as possible.

The third challenge is the fine grains and moisture in the sand. As shown in Figure 2.1, as the suction of vacuum pump is limited, one should stir the sand in the cubic recycle container by a steel shovel to make the sand be transported towards the recycle tube successfully. It is estimated to stir the steel shovel for at least 20 times for the whole container of sand's being transported. Thus, the sand stored in the container should be shovelled for hundreds of times during days of repetitive sample preparation work. It was observed that with the sand's being shovelled, the amount of dust-like fine grains increased. Hence, it was supposed by the author that this increasing amount of fine grains could be due to the abrasion of sand particles, as a result of the steel shovel's stir. What is more, for the TU Delft sand pluviator, analogous to the mechanism of revolving door, metal panels are used to transport sand from the storage tank towards the hopper. When rotating, the scratch between the wings (metal panels) and the rotunda wall is inevitable and therefore, some sand particles could be crushed. This supposal is analogous to the sieve tests by Seo et al. (2020), according to which, it was proved that the amount of fine grains increased after an oedometer tests, due to the breakage of sand grains.

The dust-like fine grains are never ignorable as they are proved by some following tests to play an important role in the behaviour of ultimately prepared sand specimens. Therefore, it is recommended that the pluviated sand should not be recycled for too many times. Additionally, the moisture in sand is also important. As the hopper is able to store more than 50 kg of sand, it is not feasible to dry the sand by oven every time before tests. Despite that, it is recommended to check the sand regularly to make sure that there is no water retention in sand at least. Sample preparation work in a humid day is not suggested.

As these indexes that challenge the standardization of sample preparation work cannot be controlled or even quantified easily, they were not set as the variables of sand pluviator's execution parameters. Despite that, these factors should always be noticed and kept generally unaltered during a certain series of sample preparation work.

<div style="text-align: right; font-size: 4em; font-weight: bold;">3</div>

Tests on the Coarse Merwede River Sand

3.1. The Coarse Merwede River Sand

3.1.1. General Description

The coarse Merwede River sand was used for preparing specimens in this work and a photograph of this sand is shown in Figure 3.1. Particle size distributions of the coarse Merwede River sand and another two well-known sands are compared in Figure 3.2 and the basic properties of coarse Merwede River sand are shown in Table 3.1.

Table 3.1: Properties of the coarse Merwede River sand

G_s	D_{60} (mm)	D_{50} (mm)	D_{30} (mm)	D_{10} (mm)	C_u	C_c	e_{max}	e_{min}
2.65	0.78	0.73	0.65	0.54	1.44	1.00	0.72	0.50

The relative density mentioned in this work is calculated by

$$D_r = \frac{e_{max} - e}{e_{max} - e_{min}} \tag{3.1}$$

where e is the void ratio of sand and its maximum and minimum values were evaluated following the Laboratory Testing Standards of Geomaterials of the Japanese Geotechnical Society (2015).

3.1.2. Shape of Sand Particles

Two-dimensional shapes of numerous coarse Merwede River Sand particles were obtained from the computed tomography (CT) images and the shapes of sand particles are evaluated.

Hitherto, no evaluation methods have been recommended by authoritative testing standards or designing codes, and the concept proposed by Zheng and Hryciw (2015) was applied in this work, which is described in Figure 3.3.

As shown in Figure 3.3, the particle shape can be characterized at three different scales. The largest scale is the form (sphericity) and it reflects the ratio of the surface area of a sphere of the same volume as the particle to the actual surface area of the particle (Wadell, 1933). The second scale is the roundness (angularity) and it reflects the ratio of the average radius of curvature of the corners of a particle to the radius of the maximum inscribed circle (Wadell, 1932). The smallest scale is the roughness, and this index is difficult to be quantified, due to the limited resolution of CT scanning and the "coastline paradox".

The sphericity is quantified by calculating the eccentricity of the ellipse that has the same second-moments as the actual shape of particles, based on the 2D CT images and then applying the function regionprops of MATLAB (MathWorks, 2019), eccentricity of 300 randomly selected particles were calculated and the average value is 0.72. That means the particles of the coarse Merwede River sand are generally not spherical and have distinctly longest axes, as eccentricity of a circle is 0 and that of an ellipse can never exceed 1. Therefore, it is of value to study the inclinations of sand particles and that study will be introduced in Section 3.6.

The evaluation method of roundness (Wadell, 1932) is complicated and its concept was further described in the following research (Wadell, 1935), as shown in Figure 3.4.
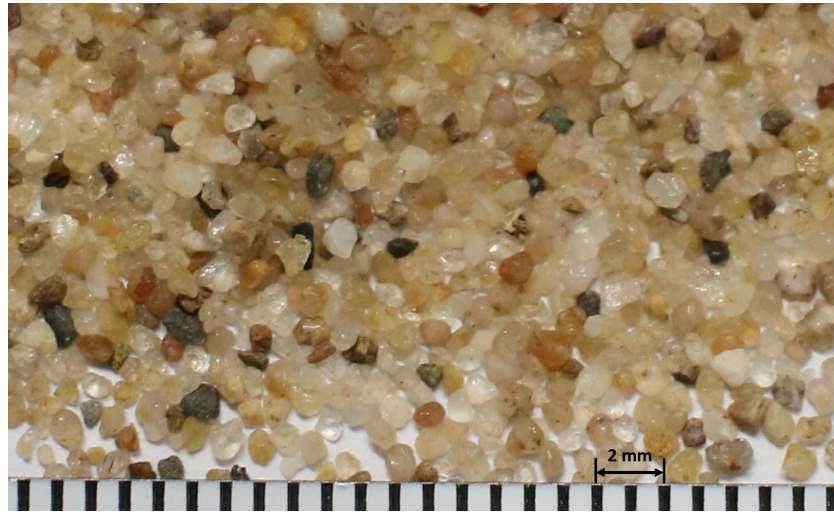
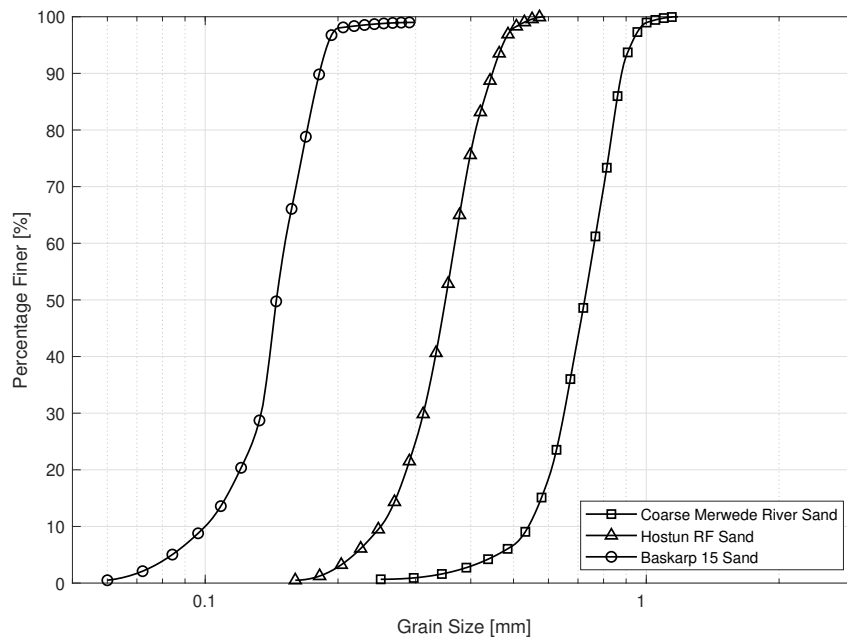Figure 3.1: The coarse Merwede River sand

Figure 3.2: Particle size distributions of the coarse Merwede River sand, Hostun RF sand (Alshibli et al., 2015) and Baskarp 15 sand (Tehrani et al., 2018)
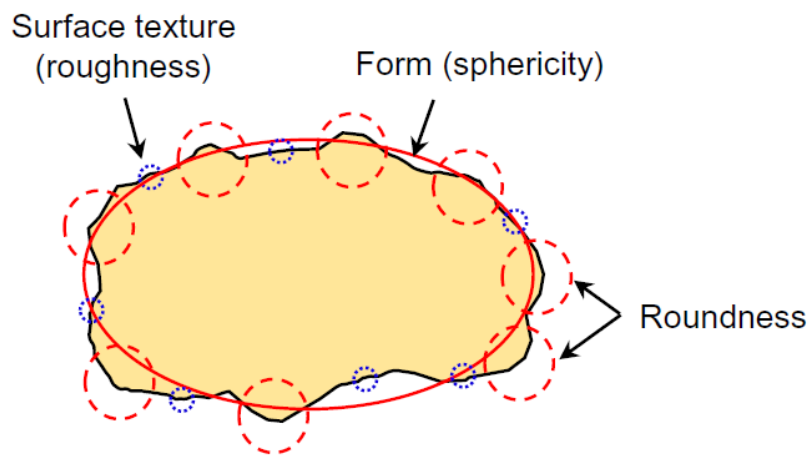
Figure 3.3: Particle shape characterisation at different scales (Zheng and Hryciw, 2015) (after Barrett, 1980; Mitchell and Soga, 2005; ISO, 2008)
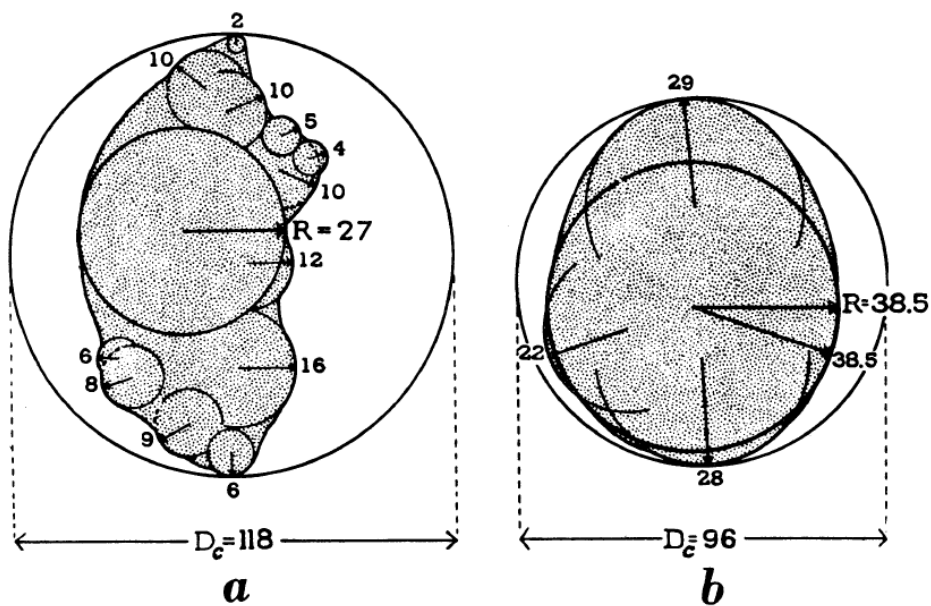

Figure 3.4: Examples of calculating the degree of roundness (Wadell, 1935)

As can be seen in Figure 3.4, the radius of the maximum inscribed circle of a particle should be calculated (abbreviated as R; for Figure 3.4a, $R = 27$; for Figure 3.4b, $R = 38.5$). Besides, radius of curvature of the "corners" of a particle (abbreviated as r; for Figure 3.4b, $r_1 = 22$, $r_2 = 28$, $r_3 = 29$) should be calculated as well. And the quantifying index of particle's roundness can be expressed as

$$\text{Degree of Roundness} = \frac{\sum_{i=1}^{N}(\frac{r_i}{R})}{N} \tag{3.2}$$

where N is the number of "corners" depicted by arcs. Partially based on this concept, Powers (1953) proposed an empirical scale of six roundness classes (e.g. very angular, angular, subangular) and one can evaluate the roundness empirically comparing the particles with reference photographs. Additionally, based on the same concept, Zheng and Hryciw (2015) proposed an algorithm to reckon the values of roundness precisely based on computational geometry and simultaneously provided the open-sourced codes.

Ultimately, the roundness of the coarse Merwede River sand was considered as "subangular to subrounded" according to the empirical method by Powers (1953) and the degree of roundness was calculated to be around 0.5 based on the concept of Wadell (1932, 1935) and its computational algorithm by Zheng and Hryciw (2015).

Overall, the coarse Merwede River sand is uniform, coarse, non-rounded, non-spherical and of various colours, and these features make it suitable for digital (photograph and CT) image analysis.

3.2. Sample Boxes

For this study, sample boxes should be specially designed. As shown in Figure 3.5, For the line-style sand pluviatiors, the width of "sand curtain" should be larger than that of sample boxes, and therefore, some sand particles my hit the top of the boxes' boundaries and then bounce off. Some of the bounced particles may fall outside the boxes while some others may fall inside and accumulate near the boxes' boundaries.

Therefore, the sharp edges must be assembled to conventional sample boxes for physical modelling, to make all the particles hitting the top of boxes' boundaries bounce outside the box, as shown in Figure 3.5. Besides, for the macro-CT scanning, the material of sample box was chosen to be wood rather than metal, to make the X-ray penetrates the box more "easily".

3.3. The Relative Density Tests

A series of sand pluviation tests were carried out using the coarse Merwede River sand and the test results are plotted in Figure 3.6. It can be seen from the figure that by adjusting the Falling Height, Opening Width and Box Speed, sand samples of various relative density (ranging from 50% to 100%) were prepared.

For each combination of variables, at least two repetitive pluviation tests were done and both results were recorded if the difference between the them is smaller than 5%, as it was stated in Chapter 2 that the errors could be larger than 10% due to the challenges. The raw data of D_r are shown with the dash curves in Figure 3.6. Additionally, the raw data were fitted for a better view of trends, as shown with the solid curves with markers.

The most general principle concluded from Figure 3.6 is that a sand sample tends to have higher relative density when the Falling Height increases or the Opening Width (positively correlated with depositing intensity) decreases, although some exceptions can be observed. This conclusion basically agrees with previous research works (e.g. Butterfield and Andrawes, 1970; Lo Presti et al., 1993; Madabhushi et al., 2006; Hakhamaneshi et al., 2016; Hossain and Ansary, 2018).

The influence of the variable Box Speed has an evidently non-monotonic feature: when the Falling Height is smaller than 50 cm, the relative density is positively correlated with the variable Box Speed while the correlation would become elementally negative when the Falling Height is larger than 50 cm. This conclusion could mediate the contradictory results from previous papers which held the views that the relative density is negatively (e.g. Stuit, 1995) and positively (e.g. Bolouri Bazaz et al., 2018) correlated with the moving speed of sample box, respectively.

Studying the detailed process of sand pluviation is a sophisticated combination of aero dynamics, impact mechanics, stochastic process, bifurcation theory and even statistical mechanics and hence the relationships among the relative density and the three variables cannot be explained scientifically at the present stage. However, a partially substantiated hypothesis of the three variables' influences on the relative density is proposed in Section 3.5.
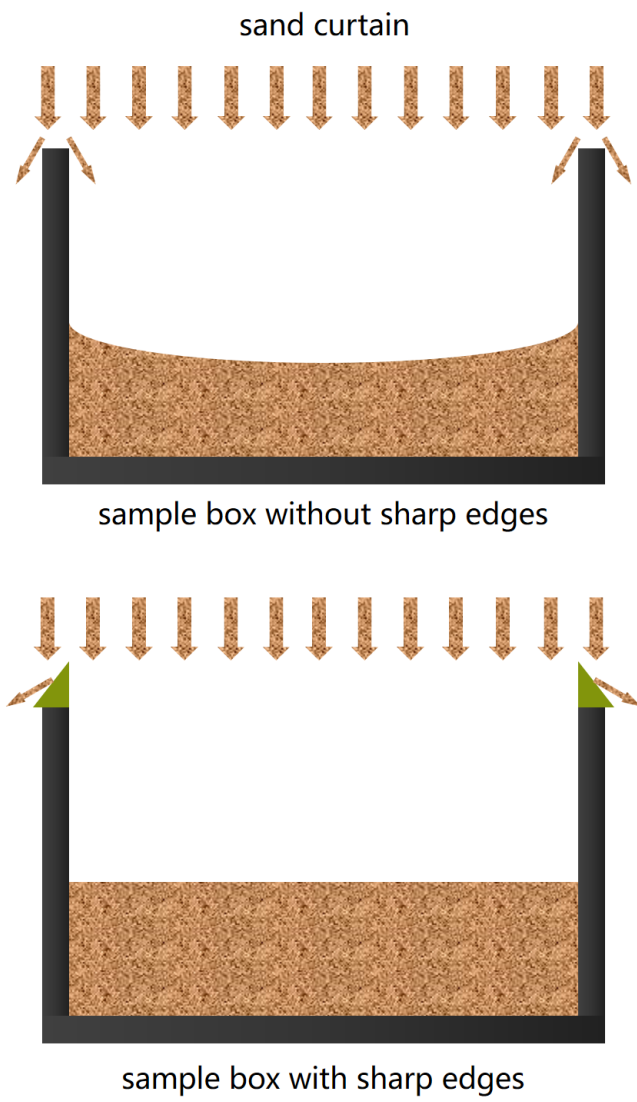
sand curtain

sample box without sharp edges

sample box with sharp edges

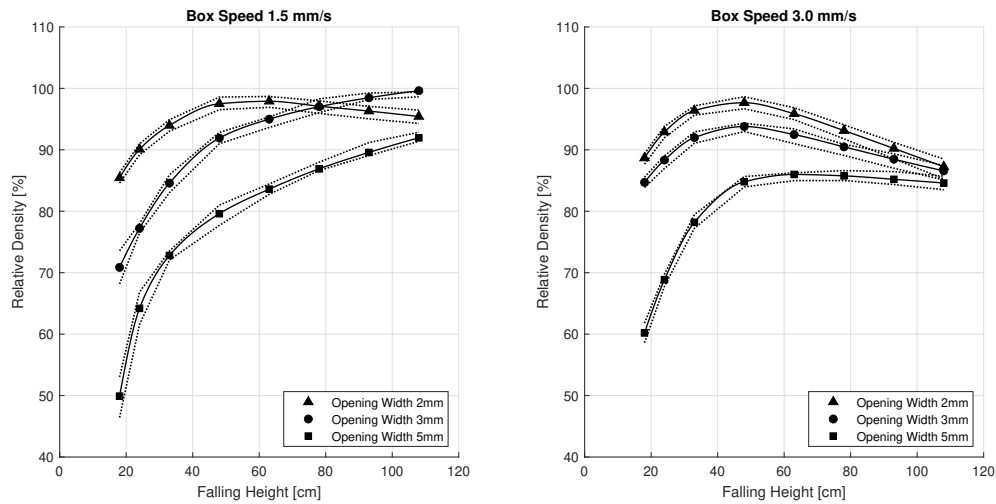Figure 3.5: Sample boxes with and without sharp edges

Figure 3.6: The relative density test results for the coarse Merwede River sand

3.4. Homogeneity Check for Pluviated Specimens

As previously mentioned, it has been proved that sand specimens prepared by the pluviation method could be heterogeneous. Besides, as can be seen in Figure 3.6, to obtain a sand sample with a certain relative density, there are usually more than one combination of sand pluviator's execution parameters that can be chosen. For example, using the coarse Merwede River sand, to prepare a specimen whose relative density is about 90%, one can set the Opening Width as 5 mm, Falling Height as 98 cm, Box Speed as 15 mm/s, or set the Opening Width as 3 mm, Falling Height as 27 cm, Box Speed as 30 mm/s. As these samples with the same relative density could have different spatial distribution of local compactness (e.g. different thickness of distinct denser and looser layers), the homogeneity of specimens must be checked by the previously introduced macro-CT.

The solved matrices of local radiographic density are shown in the form of grayscale images, see Figure 3.7 and Figure 3.8, where a smaller value of grayscale represents a smaller value of specimens' local void ratio (in other words: the darker, the denser). Besides, for convenient visualization of the alteration of the local relative density in the horizontal and vertical directions, the values of local relative density of sand packing located at the position corresponding to each pixel were back-calculated by

$$D_{r,ij} = \bar{D}_r \cdot \frac{\bar{f}}{f_{ij}} \tag{3.3}$$

where f_{ij} and $D_{r,ij}$ are the grayscale and the local relative density located at a certain position (i for column, j for row) in a CT section, respectively. $\bar{D}_r$ is the bulk relative density of a whole specimen, being calculated based on the direct measurement of sand packing's mass and volume. $\bar{f}$ is the average value of the whole section's grayscale. It should be noticed that the values of back-calculated local relative density are not necessarily the actual ones, except the mean values. However, as explained in Chapter 1, this simplified qualitative method is competent enough for the analysis of this work.

Eight specimens were scanned and four typical ones of them are shown in this chapter. Information of the four samples is shown in Table 3.2.

Table 3.2: Information of Sample 1, 2, 3 and 4

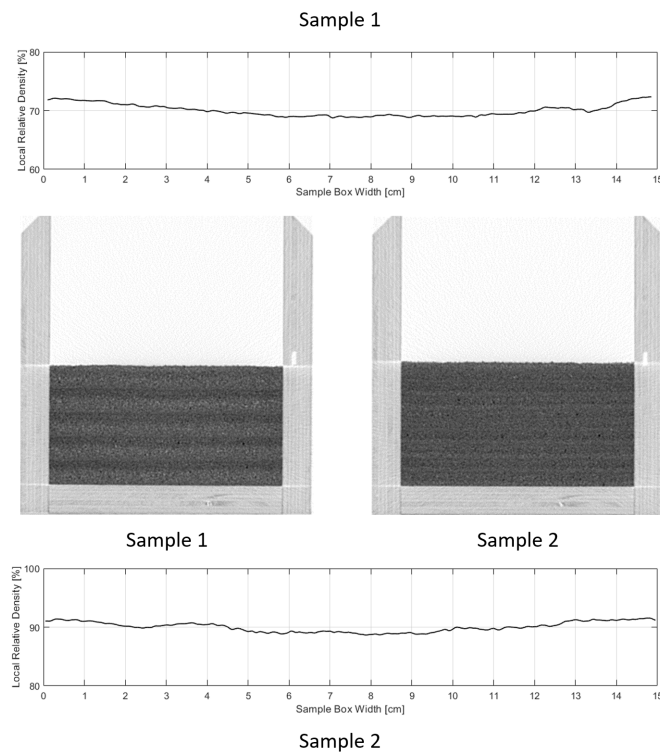|	Variables			Relative Density
	Falling Height	Opening Width	Box Speed	
Sample 1	220 mm	5 mm	30 mm/s	68%
Sample 2	280 mm	2 mm	15 mm/s	91%
Sample 3	240 mm	3 mm	15 mm/s	80%
Sample 4	480 mm	5 mm	15 mm/s	81%

Figure 3.7: Homogeneity check in the horizontal direction

3.4.1. Horizontal Homogeneity Check

The reconstructed images of Sample 1 and Sample 2 are shown in Figure 3.7. As can be seen from the curves, sand in the central part of the box is looser than that near the boundary, regardless of the vertical position. On the other side, the variation of local relative density in the horizontal direction is not as manifest as that in the vertical direction, as shown in the grayscale images of the same figure, where distinct denser and looser layers can be seen.

3.4.2. Vertical Homogeneity Check

The CT images of another two selected samples (Sample 3 and Sample 4) which have similar height and almost the same bulk relative density are shown in Figure 3.8. It can be seen from Figure 3.8 that for Sample 3, the value of local relative density varies more frequently than that for Sample 4, in the vertical direction. What is more, the coefficient of variation for Sample 3 is smaller than that for Sample 4.

All the eight scanned specimen showed the stratifying feature of "dense-loose-dense", although the thickness of different specimen's layers varies significantly. It should also be noted that the surface of a specimen is always looser than average and the surface is often the loosest part, agreeing with previous studies (e.g. Fretti et al., 1995; Choi et al., 2010).

Meanwhile, it is worth mentioning that the periodic distribution of local relative density is summarily analogous to some trigonometric functions (e.g. the sine function, which has three factors: Phase, Frequency and Amplitude). According to the eight scanned specimens, it can be concluded that the factor Phase (average D_r) is governed by the variable Falling Height; the factor Frequency (layer thickness) is governed by the variable Opening Width and the factor Amplitude (variation of D_r) is governed by the variable Box Speed. If a specific stratifying condition is needed for a sand specimen, one can try to adjust the three variables of sand pluviator to "concoct" the shape of the vertical distribution curve of local D_r. The mechanism of three variables' influences on the local relative density is described in the partially substantiated hypothesis introduced in Section 3.5.
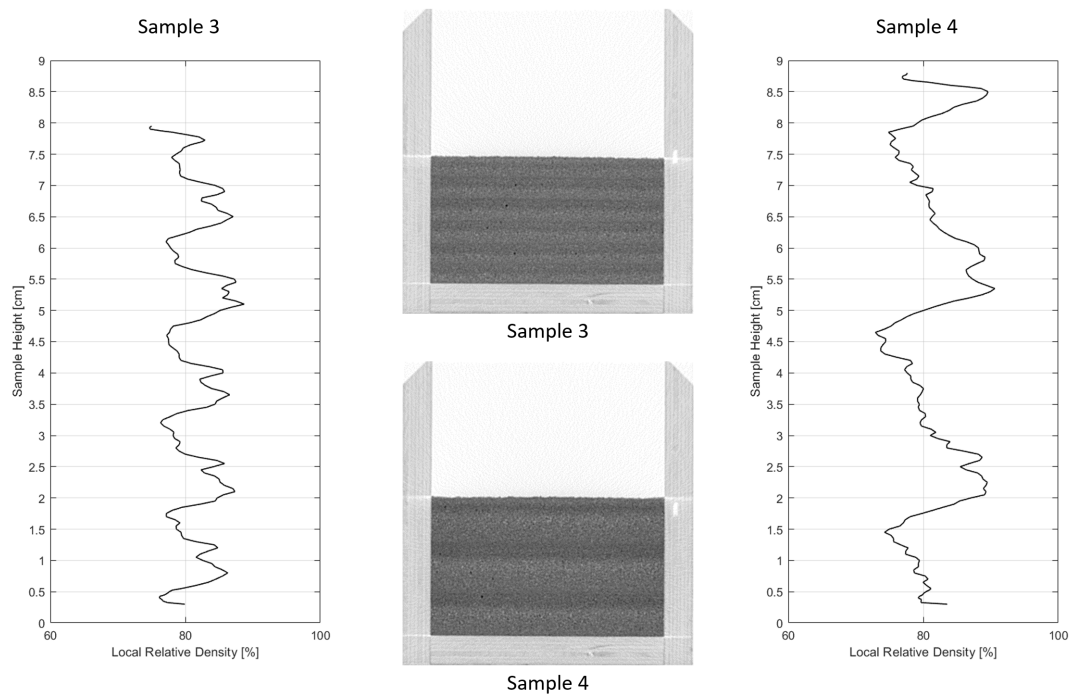
Figure 3.8: Homogeneity check in the vertical direction

3.5. Influences of Sand Pluviation Variables – A Hypothesis

3.5.1. Mechanisms of the Sand Pluviation Process

Observation through the transparent sides of the sample box agreed with the mechanisms proposed by Stuit (1995) and Cresswell et al. (1999), and the sketch of their proposed mechanisms in shown in Figure 3.9.

As can be seen in the sketch, the pluviation process can be divided into three mechanisms. The sand directly beneath the middle of hopper's bottom gap is compacted by the new falling sand grains and that is the compacting mechanism (marked red in Figure 3.9, as an additional indicator for full-colour printed version only, ditto) and the pluviated sand grains governed by which has negligible movement comparing with those governed by the other two mechanisms. As shown in the left-hand side of Figure 3.9, when the bottom gap of sand hopper is relatively large (e.g. wider than 5 times the D_{50} of stored sand), the "sand curtain" will be thick. In this occasion, a large amount of fallen sand grains roll and slide towards two sides of the curtain's section, and that is the rolling mechanism (marked green in Figure 3.9). Additionally, as shown in the right-hand side of Figure 3.9, when the "sand curtain" becomes thinner, the rolling particles will be fewer and the bouncing-off behaviour of particle becomes manifest instead, and that is the bouncing mechanism (marked blue in Figure 3.9).

According to the observation by still photographs with a shutter speed 50 frames per second, it is suggested that these three mechanisms are not incompatible and a novel "composite mechanism" is proposed, referring to the mechanisms of Stuit (1995) and Cresswell et al. (1999), as shown in Figure 3.10.

As can be seen from the sketch, after the sand curtain's hitting a former sand layer, the falling particles (marked yellow) will be divided into 3 parts, being governed by the bouncing mechanism (marked blue), compacting mechanism (marked red) and rolling mechanism (marked green), respectively. Due to the relative movement between the sand curtain and the sample box, there is usually a sand slope and the rolling mechanism is the dominant mechanism in this region. Particles governed by the rolling mechanism have no impulse left and hardly compress each other either, and thence these particles are deposited in a loose packing (Stuit, 1995).

The slope made of rolling particles is then compacted by the following falling particles and the top part of the slope is governed by the compacting mechanism by which the loose sand suffers a hammering action brought by the falling grains (Cresswell et al., 1999) and according to the CT scanning comparison, this hammering action may result in the densification of loose sand packing. In this case, a relative thin and dense layer forms, as that marked red in Figure 3.10. It is also indicated by the CT scanning comparison that only
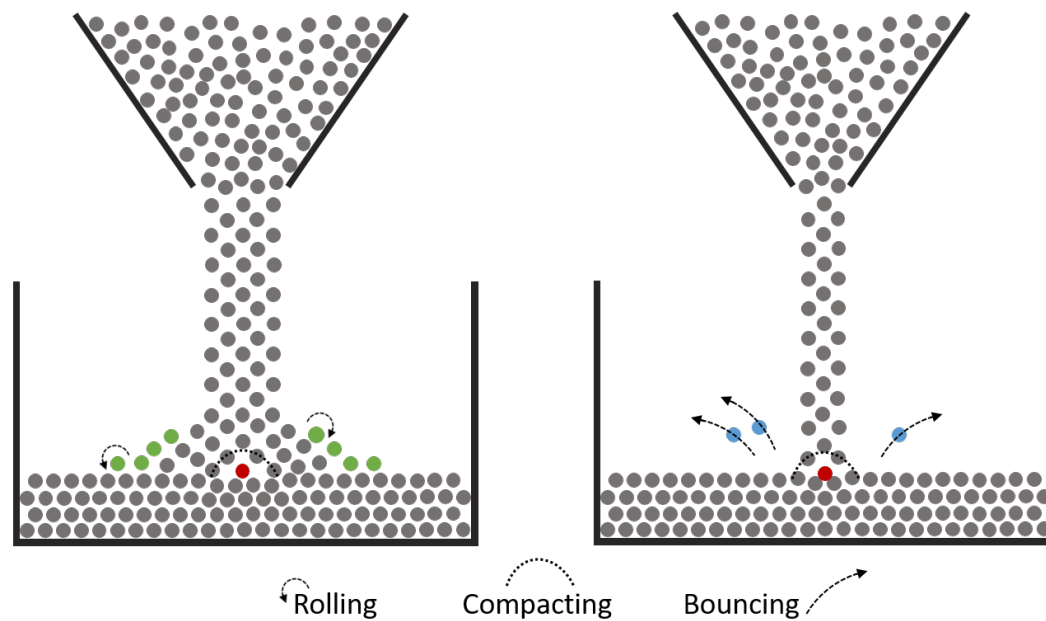
Figure 3.9: The rolling, compacting and bouncing mechanism after Stuit (1995) and Cresswell et al. (1999)

the top part (usually less than 1/3) of the loose sand packing can be compacted to be dense by the falling sand particles and the void ratio of the rest part remains almost unchanged after a sand layer's being deposited.

The bouncing off particles will fall again and then form a loose layer, as that marked blue in Figure 3.10. According to the CT scanning results (see e.g. Figure 3.8), this layer is often the loosest layer of the whole sample, but its top part will be compacted to be denser if a new sand layer would be pluviated above.

3.5.2. The Influence of Falling Height

Although the influence of air drag is not ignorable, the terminal velocity of a single falling sand particle is positively correlated with the falling height in the interval 0-1 metre (Vaid and Negussey, 1984; Chian et al., 2010). Besides, as the kinetic energy ($K.E.$) can be expressed as Eq. 3.4 (Coriolis, 1832)

$$K.E. = \frac{1}{2} m v^2 \tag{3.4}$$

where it can be seen that the kinetic energy that one sand grain has just before it hits the previous sand layer is positively correlated to its terminal velocity and therefore thus, the kinetic energy of a falling sand grain increases with it falling height, although not linearly.

According to the composite mechanism proposed in Sub-section 3.5.1, the effect of the loose (rolling) sand packing's being compacted is related to the energy of falling grains and the top part of the loose sand is hammered to be denser by falling grains with higher kinetic energy. Consequently, a sand specimen's relative density increases with the variable Falling Height in certain intervals, as can be seen in Figure 3.6. According to the CT scanning results, in this case, the increase in local relative density is more significant in the dense layer which is governed by the compacting mechanism and thence, the variation of local relative density becomes larger.

However, when the value of the variable Falling Height is large to a certain extent, the kinetic energy of the falling sand is also considerably large, and in this case, as observed from the photographs, the bouncing mechanism becomes more dominant than the compacting mechanism and thence the bulk relative density of a specimen will decrease, as can be seen in Figure 3.6 (e.g. for Box Speed 3 cm/s, Opening Width 2 mm, Falling Height > 50 cm). According to the CT scanning results, at this "high falling" stage, comparing with samples with lower Falling Height, the local relative density of the compacted dense layers decreases while the previously loose layers are densified. Consequently, the variation of local relative density decreases and the sand specimen becomes more homogeneous in terms of the void ratio.
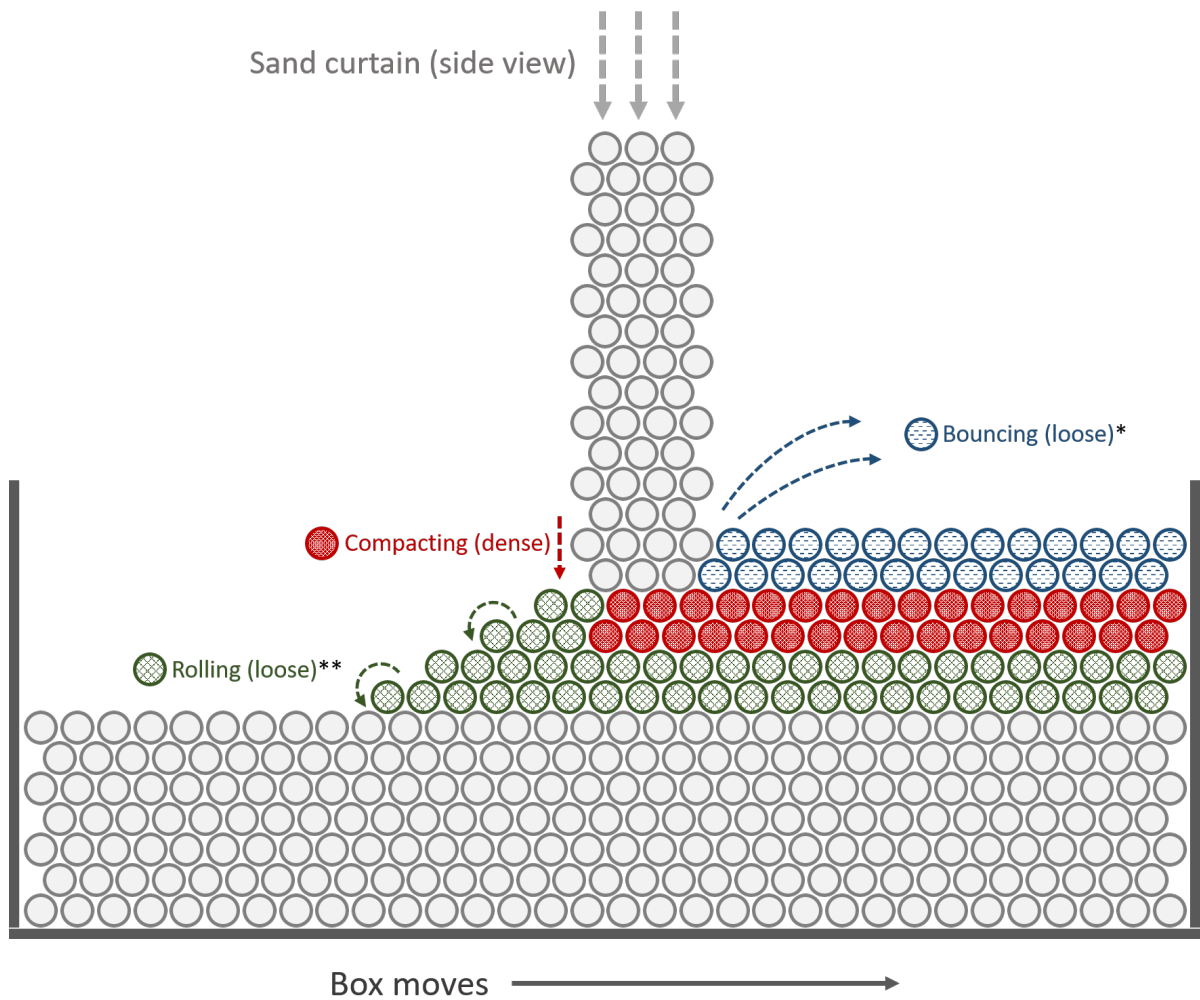
Figure 3.10: The composite mechanism

* The layer governed by the bouncing mechanism should be loose, especially when comparing with that of compacting mechanism. However, the bouncing layer is densified if a new layer is pluviated above.

** Some particles may bounce to this area. However, to make the figure tidy, the bouncing mechanism is not shown here together with the rolling mechanism, as they have the similar effect to make the sand packing loose.

3.5.3. The Influence of Opening Width

It was observed that with a larger value of Opening Width, the thickness of each layer becomes larger, because of the positive correlation between the width of the opening gap and sand's depositing intensity. According to the results of high frame rate photographing, when the opening gap becomes wider, the main growth in sand layers' thickness is for the loose layers governed by the rolling mechanism (marked green in Figure 3.10). That is the reason for the relative density's basically monotonic decreasing with a wider opening gap of the sand hopper.

Additionally, if a combination of three variables for a relative loose sand sample is in need of being improved to make a denser sample, it is not wise to increase the Falling Height recklessly, with a large Opening Width unchanged, because that would make the differences of relative density among layers larger. Taking priority selecting a smaller value of Opening Width is a better choice instead.

3.5.4. The Influence of Box Speed

It was observed that the reasons for the growth in sand layers' thickness is not only large Opening Width, but also lower Box Speed. The influence of Box Speed on thickness of layers is not as significant as that of Opening Width because the interval of appropriate values of Box Speed is not wide. For example, a box's moving speed cannot be very slow, otherwise one would get a sand dune in the box; or very fast, otherwise sand specimen would be disturbed by the high acceleration.

Analogous to the reasons for looser samples due to large Opening Width, low Box Speed will make the loose layers which are governed by the rolling mechanism thicker, resulting in the decrease of the bulk relative density. However, if the Falling Height is large (see e.g. in Figure 3.6, for Opening Width 3 mm, Falling Height > 50 cm), with a higher Box Speed, the loose layers governed by the rolling mechanism will be thin and hence the dense layers which could have been governed by the compacting mechanism start bouncing off because of the high kinetic energy due to the large value of Falling Height. As the compacted dense layers are difficult to form and therefore, the relative density decreases with a higher Box Speed in these "high falling and high speed" intervals.

3.5.5. Practical Recommendations Based on the Hypothesis

Although cannot be proved prudently by mathematical methods, the proposed composite mechanism of sand pluviation is considered as rational according to the high frame rate photographs and CT scanning results. Based on this the partially substantiated hypothesis, the following recommendations are proposed.

For specimens prepared by the TU Delft sand pluviator using a certain type of sand, the relative density has a generally similar relationship with the Falling Height, regardless the values of Opening Gap and Box Speed. And the curve representing that relationship can be divided into four phases, as shown in Figure 3.11.

The Phase 1 is for the loose specimens prepared with a very small value of Falling Height (e.g. less than 20 centimetres). As explained in Chapter 2, the parameter Falling Height can never be smaller than the height of sample boxes and thence, it is difficult to prepare loose samples (e.g. $D_r < 40\%$) by a line-style pluviator and consequently the Phase 1 is usually missing. When turning into Phase 2, the relative density still increases rapidly with a growing falling height, as it did in Phase 1. In this phase, the dense sand layers governed by the compacting mechanism start to become distinct and a periodic variation of D_r along depth becomes manifest. In Phase 3, the relative density increases mildly comparing with the first two phases and the bulk relative density in this phase is typically larger than 70%. It is noticeable that the variation of local relative density in this phase is the largest among four. In other words, in this phase where the bulk relative density increased from 70% to 90%, the D_r of originally denser layers increase even faster than that of originally looser layers, until the denser layers reach the state of the minimum void ratio. In the last phase, Phase 4, the Falling Height is usually larger than 50 centimetres. Falling particles with high kinematic energy make the bouncing mechanism more prevalent than the compacting mechanism and hence the relative density decrease after reaching the peak. In this phase, the variation of local relative density becomes considerably small and the most homogeneous specimens can be made. Besides, it is worth noting that the relative density is more difficult to control comparing with the previous phases, as the bouncing mechanism is predominant and the grains' collision is a stochastic process which is sensitive to the challenges mentioned in Chapter 2 (i.e. fullness of sand hopper, initial state of stored sand, dynamic abrasion of sand particles).

Generally, for preparing sand specimens by the TU Delft sand pluviator, a small value of Opening Width (e.g. less than five times the D_{50} of sand) and a relatively large value of Box Speed (e.g. 3 cm/s) are recommended. With this indication, specific values of the variables Opening Width and Box Speed should be tentatively chosen, then one should try to plot the curve showing the relationship between the variable Falling
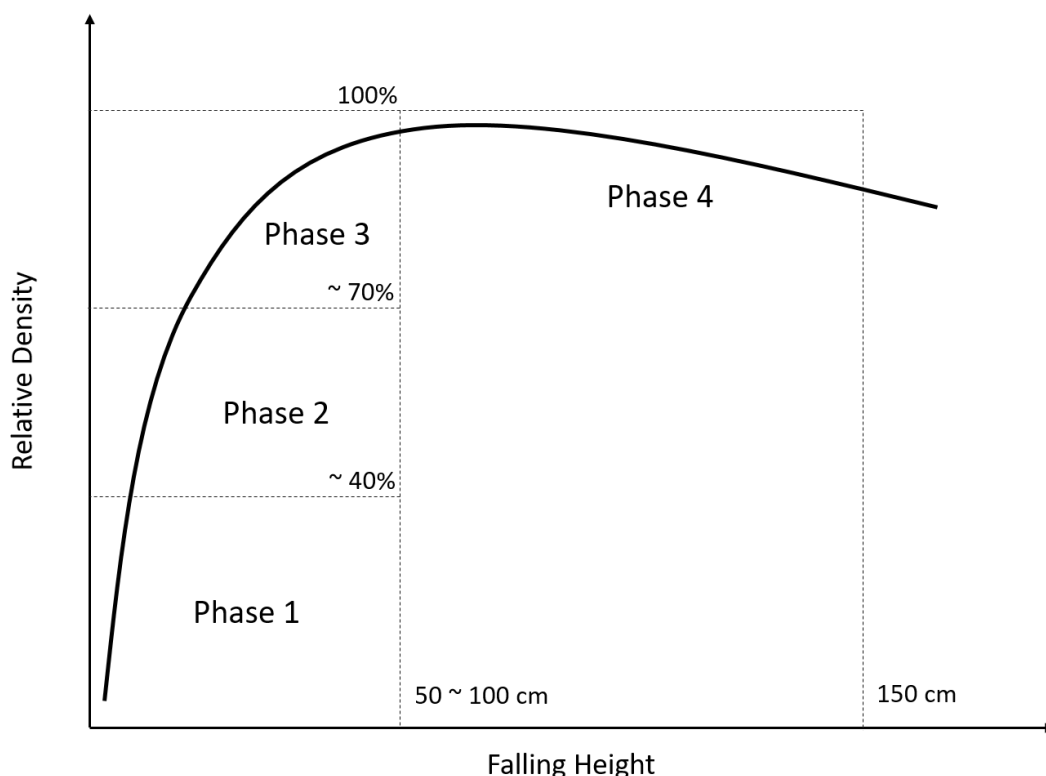
Figure 3.11: Falling-height-dependent phases of sand pluviation: a general rule

Height and the ultimate bulk relative density, referring to a series of (usually four or five) pluviation tests adjusting the Falling Height. Then, the plotted curve should be divided into three phases (i.e. Phase 2, 3, 4, as Phase 1 is usually missing) referring to Figure 3.11. Phase 2 and Phase 3 are not recommended if one is fastidious about specimens' uniformity, especially the latter phase, as the value of relative density of whom coincides with that of Phase 4. The Phase 4 is strongly recommended, although only very dense (usually D_r > 80%) samples can be made in this phase.

If a very dense sample is planned, and Phase 2 exists in the plotted curve, one should narrow the Opening Width and increase the Box Speed to make Phase 2 disappear in the newly plotted curve. As long as Phase 2 disappears, the setting of variables Opening Width and Box Speed should be fixed and then one can choose a proper Falling Height in Phase 4 to prepare a specimen with a targeted value of D_r.

On the other hand, for a sand sample whose D_r is smaller than 70%, one should set the value of Falling Height as small as possible and carefully increase the Opening Width and slow down the Box Speed, until a targeted D_r is reached. Although would result in the evidently periodic variation of local D_r along depth, this approach is indeed the best one among many.

In terms of homogeneity of particles' compactness, the conventional pluviation method is hardly an ideal one comparing with the vibration method, as the layering feature is manifest unless the sample is very dense, and the very high values of relative density is not frequently chosen for physical modelling. Besides, it is almost impossible to prepare loose samples by the pluviation method, especially using the line-style pluviators. Despite this, it is not recommended by the author that the pluviation method should be abandoned as it has its great advantage of rational inclination of sand particles and this point is introduced in Section 3.6. To solve the defects mentioned above, instead of the traditional dry pluviation method, the air-water pluviation method can be an alternative. As shown in Figure 3.12, a layer of water covering previously pluviated sand layers is indispensable and hence the falling sand particles are dragged by water. In this occasion, the composite pluviation mechanism proposed in this chapter becomes not applicable and the new mechanism is in need of being investigated. Although having not been checked by CT scanning in this work, the air-water pluviation method was proved to be able to make looser and more uniform sand specimens (Vaid and Negussey, 1984, 1988; Wijewickreme et al., 2005). Therefore, the air-water pluviation method is strongly recommended for further research.
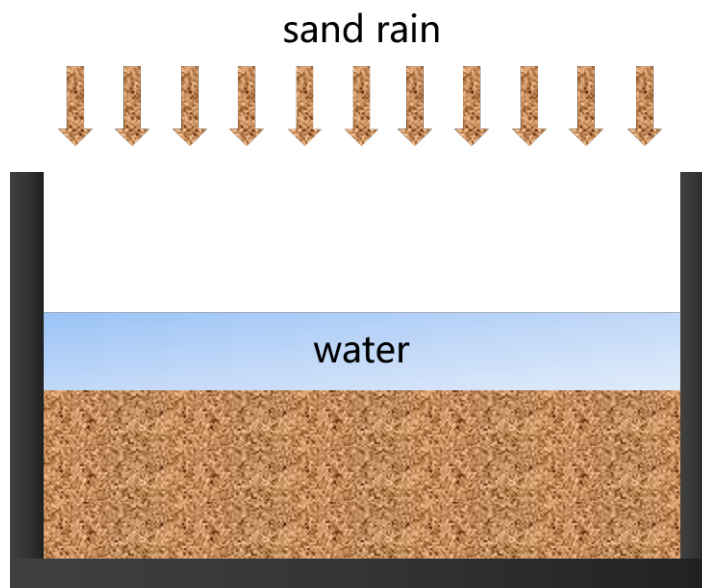
Figure 3.12: The air-water pluviation method

3.6. Fabric Features of Pluviated Specimens

3.6.1. General Description

Shapes of sand particles can be seen in the reconstructed tomographic images, as shown in Figure 3.13, where brighter pixels represent materials with higher radiographic densities (i.e. silica sand grains and metal impurities, rather than air or water).

The micro-CT image shows the fabric features of the sand specimen and the layers governed by different pluviation mechanisms are clearly indicated as well, following the hypothesis introduced in Section 3.5. As marked in Figure 3.13, the sand of the rolling mechanism is indeed loose as the ratio of area taken by sand grains is obviously small.

Besides, it is notable that in the area of the compacting mechanism, pixels representing void are brighter and that is due to the water retention. As explained in Figure 1.4, the small samples for micro-CT scanning are made from the frozen samples and thence some water was not thoroughly drained, retaining among particles. It was observed by Khaddour et al. (2018) that the amount of local water retention in sand is negatively correlated with local porosity. Therefore, the brighter pixels can be considered as the indication of locally accumulated fine grains and dust (grains finer than 0.1 mm, which could have been cleared) which provides small porosity for water retention. The dust cannot be clearly depicted by the micro-CT scanner but it indeed exists according to previous optical observation.

As a comparison, as shown in Figure 3.14, here is no obvious local accumulation of fine grains or dust for the specimen prepared by the traditional vibration method. Besides, in the CT image of the vibrated specimen, one cannot see manifest stratifying condition which is a significant feature of pluviated specimens.

3.6.2. Quantification of Fabric Features

More than general descriptions, quantification of fabric features is needed to evaluate the specimen prudently. This work focus on two aspects and they are local grain size distribution and orientations of sand particles, respectively. It was planned to quantify the fabric features using the index coordination number, which is popular in the field of DEM, to estimate the stability of clusters of idealized spheres. However, as it has been revealed that the 2D coordination number is generally positively correlated with the 3D coordination number for granular materials (see e.g. Rabbani et al., 2016) and negatively correlated with porosity (see e.g. Smith et al., 1929) and therefore, the index coordination number reflects the similar information as that represented by the relative density, which has been discussed in details in the previous sections. What is more, it has been indicated that the index coordination number cannot represent the mechanical response of granular materials if the form, roundness and roughness of particles are not taken into account (see e.g. Rorato et al., 2018). Therefore, the index coordination number was not used to quantify the stability of sand
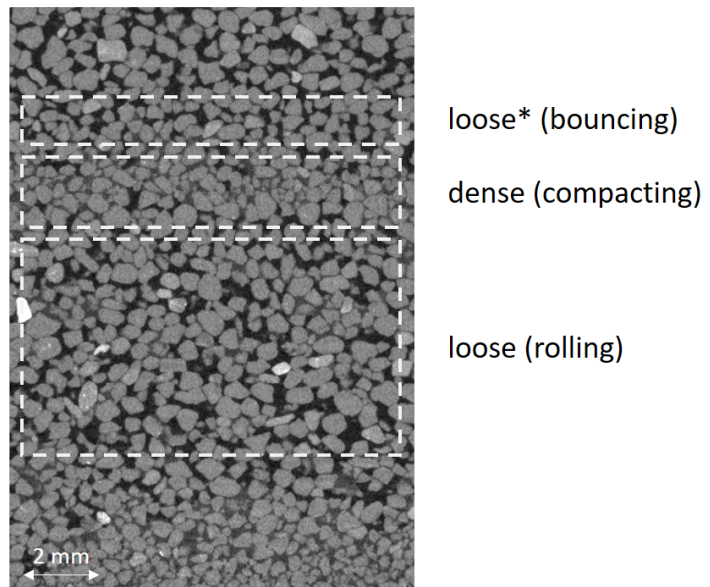
Figure 3.13: Micro-CT of sample D01 by the pluviation method

* Same as the illustration of Figure 3.10: the layer governed by the bouncing mechanism should be loose, especially when comparing with that of compacting mechanism. However, the bouncing layer is densified if a new layer is pluviated above.
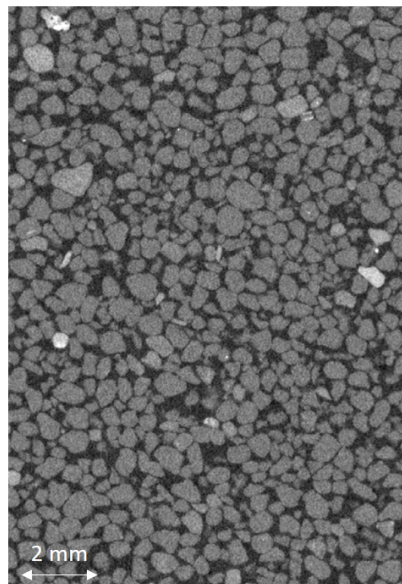

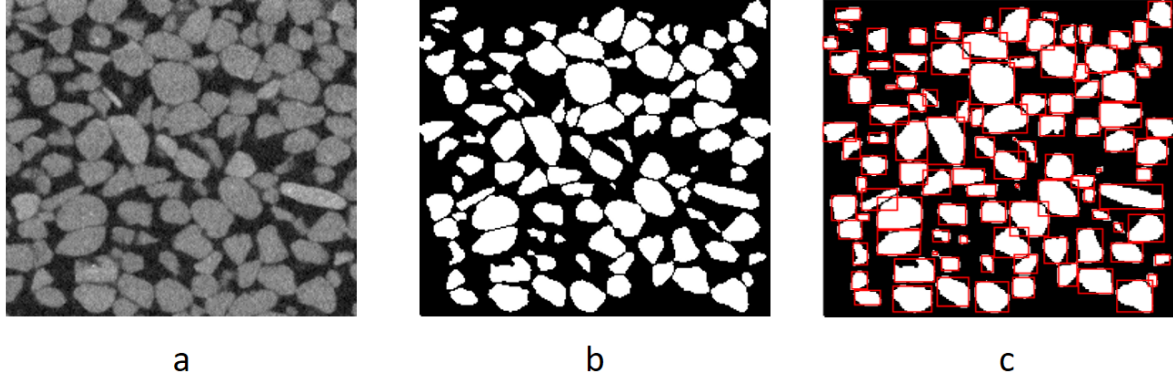Figure 3.14: Micro-CT of sample Y01 by the vibration method

Figure 3.15: Image processing steps for extracting particles (a. grayscale image; b. binary image; c. particle detecting)

packing.

In this study, recognizing and segmenting sand grains from the CT images are necessary, the Image Processing Toolbox of MATLAB (MathWorks, 2019) were applied to carry on with these works, and the processing steps are shown in Figure 3.15.

Firstly, the reconstructed grayscale CT image is binarized using a certain threshold and the value of threshold was dynamically determined by the author referring to optical observation. Afterwards, when distinct sand particles can be clearly shown in the binary image, the function reigionprops of MATLAB was used to extract each single particles, and the particles with bounding boxes are shown in Figure 3.15c. It should be mentioned that during the process of binarization, some of the sand grains can be "bonded", the function watershed of MATLAB was used to segment those grains, although the particles could be over-segmented (an integral particle is split into multiple smaller pieces) and this phenomenon agrees with that mentioned by Andò et al. (2013). Therefore, the binarization work should be partially artificially executed. In other words, one can segment the bonded particles by changing the values of certain pixels directly.

To describe the orientation of a packing of sand particles, the method for analyzing the two-dimensional orientations of geological features proposed by Curray (1956) was applied, and it can be expressed as

$$\bar{\theta} = \frac{1}{2} \arctan \frac{\sum n_i \sin 2\theta_i}{\sum n_i \cos 2\theta_i} \qquad (3.5)$$

$$L = \frac{100}{\sum n_i} \sqrt{(\sum n_i \sin 2\theta_i)^2 + (\sum n_i \cos 2\theta_i)^2} \qquad (3.6)$$

where θ_i is the azimuth of each sand grains, $\bar{\theta}$ is the preferred orientation direction of an interested packing of sand particles, L is the magnitude of resultant orientation vector in terms of per cent, and n is the number of particles. For L, a value of 100% indicates that all the sand grains has the same inclination while a value of 0 means that the inclination of each sand grains are completely different. The inclinations of sand particles located in each areas of interest are shown in Figure 3.16 and the values of $\bar{\theta}$ and L are shown in Table 3.3.

Table 3.3: Sand particles' orientation features for different pluviation mechanisms, comparing with the vibration method

	Resultant Azimuth $\bar{\theta}$	Resultant Magnitude L
Pluviation Method	4°	27%
– Bouncing Mechanism	0°	29%
– Rolling Mechanism	2°	28%
– Compacting Mechanism	12°	22%
Vibration Method	35°	3%

As can be seen, for the sand specimens prepared by the pluviation method, here exists a tendency that particles lie horizontally and this feature agrees with previous research works (e.g. Arulanandan, 1978).

Additionally, it is notable that for the sand layers governed by the compacting mechanism, where the resultant preferred inclination of particles is larger than those of two other mechanisms and the variation of
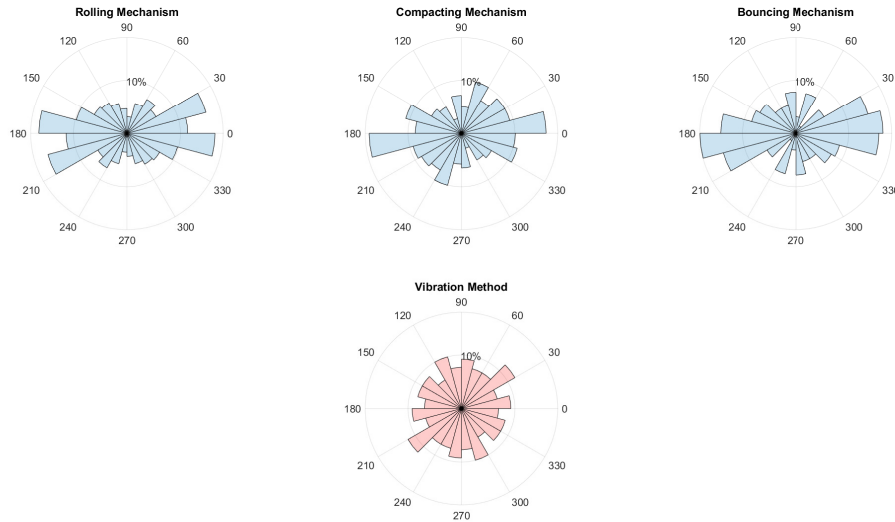
Figure 3.16: Sand particles' inclinations for different pluviation mechanisms, comparing with the vibration method
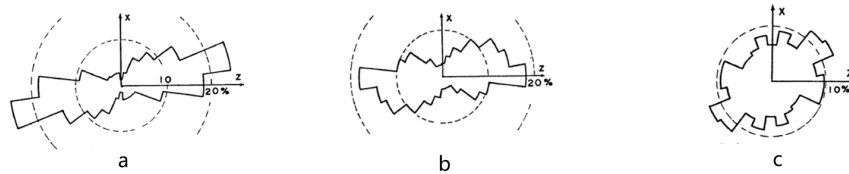

Figure 3.17: Rose diagram to show preferred orientation of sand particles of different in-situ samples in Japan (Oda and Koishikawa, 1978) (a. Fuji river sand sample No. 6; b. Kugenuma beach sand sample No. 52; c. Shirako dune sand sample No. 19)

particles' orientations is also larger for the compacting mechanism. Although the differences among the three mechanisms are relatively insignificant when comparing with specimens prepared by the vibration method, by which, more sand particles tend to stand vertically and hence the resultant azimuth of the whole sample is increased up to 35°. What is more, the small value of Resultant Magnitude L reflects the random distribution of particles' orientations for sampled prepared by the vibration method.

The preferred orientation of numerous in-situ samples was analyzed by Oda and Koishikawa (1978) using the same quantifying method, and the rose diagrams are shown in Figure 3.17. When comparing Figure 3.16 with Figure 3.17, it can be generally supposed that the pluviation method is more suitable for preparing specimens modelling river sand and beach sand while the vibration method could be relatively more suitable for modelling dune sand.

The local grain size distribution is of great significance as well, as a small amount of extra fine grains could result in evident differences in sand's behaviour. For example, specimens which were made from the same silty sand but by different preparation methods were observed to have distinct behaviour in a series of undrained triaxial compression tests (Yamamuro and Wood, 2004). One potential explanation for this phenomenon is based on the hypothesis proposed by Yamamuro and Lade (1997): a silty sand specimen would be less likely to be liquefied if large grains contact with each other directly. In contrast, if the large grains are connected by fine grains, the microstructure of silty sand would become weaker than the former one, evening having the same recipe of silt and sand. What is more, the existence of fine grains in sand changes the hydraulic conductivity of the medium along the drainage path and hence affects the hydraulic behaviour of sand, such as dissipation of excess pore water pressure (Askarinejad, 2013).

Therefore, analogously, the local grading condition of specimens prepared by the pluviation method must be taken into account, although very fine grains cannot be depicted clearly by the micro-CT scanner of TU Delft. The grain size distribution of particles in areas of different mechanisms are shown in Figure 3.18. It is conspicuous that the sand packing in the area of the rolling mechanism has generally larger grain sizes and
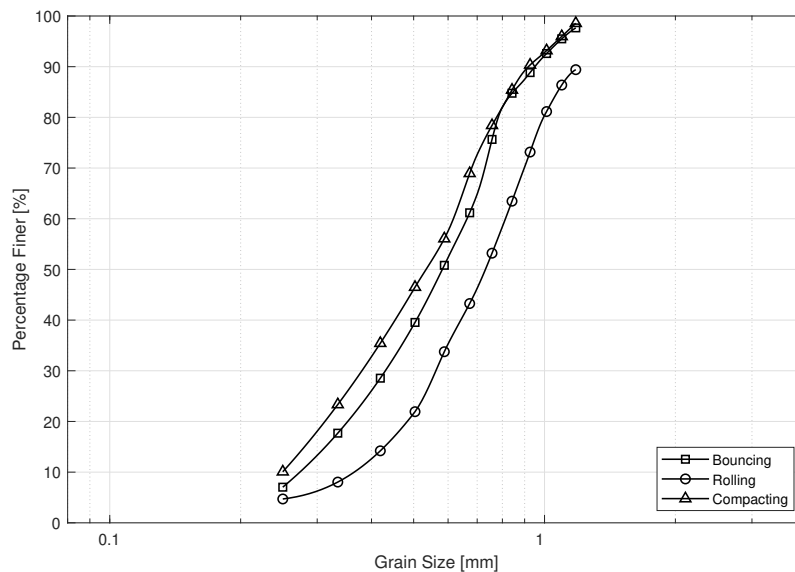
Figure 3.18: Grain size distribution of different pluviation mechanisms of the coarse Merwede River sand (based on image analysis)

this phenomenon indicates that fine grains are more likely to accumulate in the layers of bouncing and compacting mechanisms, especially the latter one. It is also worthy of mentioning that the grain size distribution curves by image analysis represents better grading condition (e.g. larger C_u) than that by the sieve analysis. It is due to the flaw of the image processing method applied in this study and this phenomenon agrees with previous works (e.g. Alshibli et al., 2015). Better grading in the area of the bouncing and compacting mechanism could result in mechanically stronger layers according to the conventional view, but it is not impossible to increase the local risk of liquefaction, especially when the fine grains are located among the large grains. Thus, the detailed contacting condition of fine grains is recommended to be observed by apparatuses with higher resolution.

3.7. Discussions on the Behaviour of Pluviated Specimens

3.7.1. The Shallow Foundation Comparison Test

To quantify the physical property of sand specimens, the relative density is undoubtedly an important and persuasive index, as it affects the behaviour of sand significantly. However, as explained before, the behaviour of sand could be affected by many other factors (e.g. inclination of particles) and it has been indicated by many researchers that sand specimens having the same relative density but different other fabric features could have significantly different behaviour for shear, compression, cone resistance and liquefaction tests (see e.g. Arulanandan, 1978) and those differences must be discussed prudently for the standardization of sample preparation work for physical modelling in geotechnics.

Merely focusing on the bulk feature of sand's fabrics is not enough. As explained in Section 3.6, for one specific pluviated sand sample, fabric features (i.e. inclination of particles and local grain size distribution) of distinct layers are different. Therefore, the expected different behaviour of pluviated specimens with the same relative density should be due to both local fabric features themselves and their spatial alteration.

Despite the complexity, a set of comparison tests were done to check the behaviour of two pluviated specimens elementally. The previously introduced Sample 3 and Sample 4 were selected, as they have the same bulk relative density (both around 80%). The preparation variables are described in Table 2.1 and the vertical distribution of local relative density is shown in Figure 3.8.

As the factor of heterogeneity has been included in many designing methods of shallow foundations (see e.g. Mayne and Poulos, 1999) and taking the relative simplicity into consideration, for these two samples, 2D strip shallow foundation tests were applied. The width of the foundation is 3 cm, which is 1/10 of the sample box's length and approximately 1/3 of the sand body's depth. The sketch of these tests is shown in Figure 3.19, and the tests were done in the centrifuge with an acceleration of 40 times gravity to simulate the condition of
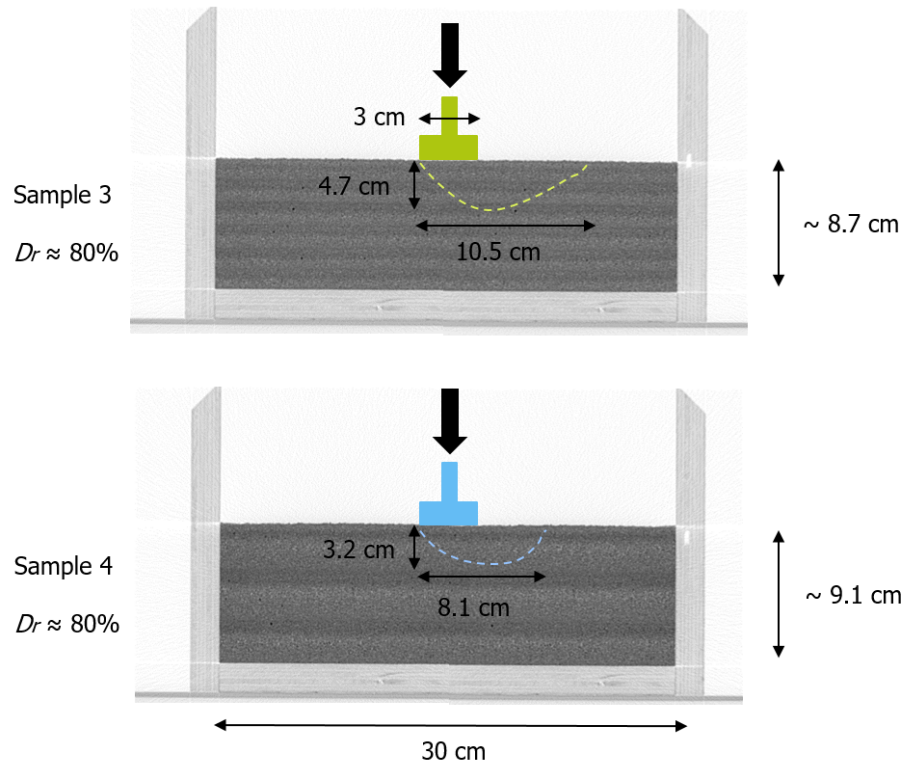
Figure 3.19: Sketch of the shallow foundation comparison test

a more realistic scale.

As shown in Figure 3.19, the sand bodies of Sample 3 and Sample 4 have the similar size and relative density but ultimately distinct shear bands. To be more specific, for Sample 3, the shear band has a depth of 4.7 cm and length of 10.5 cm, while the depth and length of Sample 4 are 3.2 cm and 8.1 cm, respectively. These distinct results are not unexpected, as many works researching on the random field of numerical modelling have indicated that the different patterns of heterogeneity may results in significantly distinct failure modes of slopes (see e.g. Hicks and Spencer, 2010) and to some extent, these conclusions are analogous to those of shallow foundation tests.

Besides, the different load-settlement curves are noticeable as well, as shown in Figure 3.20. It is worthy of mentioning that the curves are "weird" comparing with those normal ones whose value of vertical load decrease monotonically after reaching the peak. This is due to the low stiffness of the loading frame in the centrifuge. When the value of load increases, the shallow foundation model rotates, making the loading non-vertical and eccentric. That is also the reason for the existence of only one shear band for each tests, rather than symmetrical two under normal circumstances. The changing direction of loading made the shear bands developed intermittently and thence, the values of load for both Sample 3 and Sample 4 dropped instantaneously for times. Despite that, there indeed exists significant difference between the bearing capacity of Sample 3 and Sample 4. To be more specific, the peak values of load (before the first slide) of these two samples are 2502 N and 1815 N, respectively, as shown in Figure 3.20.

3.7.2. Other Discussions

In addition to the shallow foundation cases, the behaviour of pile foundations is a topic deserving discussion as well. According to the designing method proposed by the American Petroleum Institute (API) (1993), the shaft capacity of piles in sand is directly related to the average values of stress level and relative density at certain depths. That means the total bearing capacity is not sensitive to the variation of the relative density along depth and thence, the influence of the stratification condition of samples prepared by the pluviation methods could be considered as insignificant for pile foundation issues, at least for the vertical bearing capacity. However, as it has been indicated that the shaft resistance of piles can be described as a function of a set of more sophisticated parameters including the cone resistance (q_c) value of CPT tests (see e.g. Gavin and
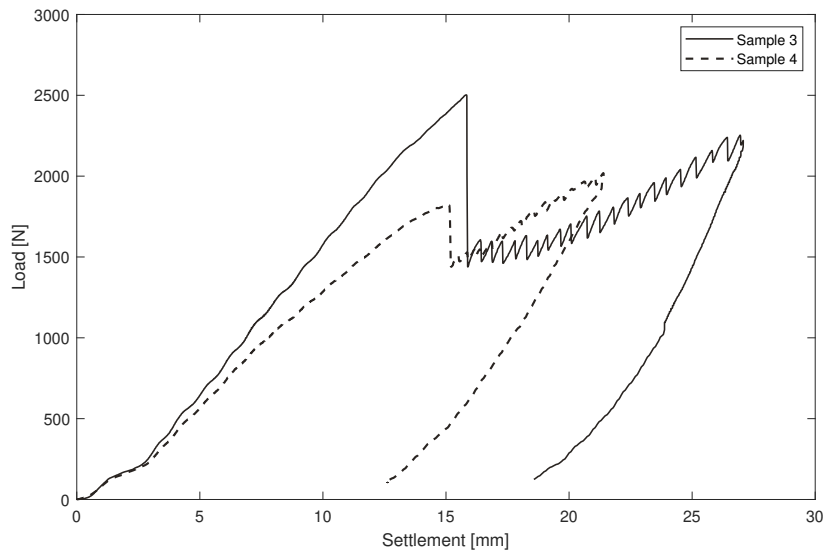
Figure 3.20: Load-settlement curves of the shallow foundation comparison test

Lehane, 2003) and hence, a series of pile installation tests or CPT tests are still recommended in the future research.

What is more, the varying value of permeability must be noticed. As shown in Figure 3.13, fine grains and dust tend to accumulate in certain layers. These layers with fine grains work as capillary barrier, as shown in Figure 3.21 where it can be seen that the horizontal saturating speed of different layers varied. It has been indicated that the hydraulic impedance caused by the capillary barriers have significant effects on the results of physical modelling tests (Mancarella and Simeone, 2012). The physical modelling project for a dike (van Adrichem, 2021) should be mentioned and for which, the influence of time-dependent change of water level on the dike was explored. It is not unimaginable that if the model (as shown in Figure 3.22) was prepared by the pluviation method and consequently have embedded dust layers, the tests results would be seriously affected by these capillary barriers, which can be considered as experimental errors.

Figure 3.21: The capillary barrier effect of a pluviated specimen

Figure 3.22: Physical modelling for the dike project (van Adrichem, 2021)

<div style="text-align: right; font-size: 3em; font-weight: bold;">4</div>

Tests on the Geba Sand

4.1. The Geba Sand

The Geba sand is used for the mono-pile's physical modeling project at TU Delft, and the pluviation method was chosen for the sample preparation work. Therefore, tests for the Geba sand should be done using the TU Delft sand pluviator.

Besides, for the sand pluviation process, a hypothesis and a series of practical recommendations were proposed in Chapter 3, and the reliability of these proposals would be checked in the tests on the Geba sand.

The basic properties of the Geba sand are shown in Table 4.1 (after Maghsoudloo et al., 2018; Krapfenbauer, 2016).

Table 4.1: Properties of the Geba sand

G_s	D_{60} (mm)	D_{50} (mm)	D_{30} (mm)	D_{10} (mm)	C_u	C_c	e_{max}	e_{min}
2.65	0.123	0.118	0.110	0.084	1.47	1.17	1.07	0.64

4.2. Sample Box

A cylinder sample box is selected for the mono-pile project. The inner diameter of the box is 295 mm and the height is 180 mm. The photo of this cylinder box is shown in Figure 4.1.

Figure 4.1: The cylinder sample box

4.3. The Relative Density Tests

For the mono-pile modelling project, using the Geba sand, samples with the relative density of 80% and 40% are needed. Following the practical recommendations based on the hypothesis, samples with satisfying relative density were prepared within a limited number of attempts, and the processes for the "D_r 40% specimens" and the "D_r 80% specimens" are shown in Table 4.2 and Table 4.3, respectively.

Referring to the previously mentioned recommendations, for the relatively loose "D_r 40% specimens", the Box Speed was initially set as a small value of 15 mm/s. The Opening Width was set as a large value of 1.0 mm, which is about 8 times the D_{50} of the Geba sand. The Falling Height was also set as a small value of 240 mm (as the minimum value is 180 mm, which is the height of the sample box). This "recipe" is recorded as Attempt 1 in Table 4.2. The D_r of the pluviated specimen was 52% and undoubtedly too dense for 40%. Therefore, the Opening Width should be increased, and the Falling Height should be decreased. As the current value of Falling Height is already very small, it was decided to increase the Opening Width to 1.5 mm firstly, as recorded in Attempt 2. As a results of the actions mentioned above, the D_r decreased to 49%, but still dense. Hence, the Falling Height was decreased to the minimum value of 180 mm for Attempt 3. If the D_r for Attempt 3 was still too high, the Opening Width would have to be increased again, although that is not beneficial to the homogeneity. Luckily, the D_r for Attempt 3 was 39%, and no further actions for the Opening Width needed to be taken.

For the relatively dense "D_r 80% specimens", the Box Speed was initially set as a large value of 30 mm/s, and the Opening Width should undoubted be smaller than the value of 1.5 mm for the "D_r 40% specimens". The Falling Height remained 240 mm for the first trial (recorded as Attempt 4 in Table 4.3). The D_r for Attempt 4 was 57%, which is smaller than the targeted value of 80%. According to the recommendations, the Opening Width should be decreased in this occasion. However, it was observed that when the Opening Width is smaller than 1 mm, the Geba "sand curtain" would become "unstable", in other word, many of the particles moved horizontally rather than fell down ideally vertically. Therefore, the Opening Width remained 1.3 mm, and the Falling Height was increase to 540 mm. Consequently, the D_r for Attempt 5 increased to 77%, which is basically satisfying. As mentioned in Chapter 2, the deviation of the relative density of pluviated specimens could exceed 5% due to the challenges, and therefore, the results of Attempt 3 and Attempt 5 are acceptable.

The tests on the Geba sand proved the reliability of practical recommendations based on the hypothesis proposed in Chapter 3. In other words, one can concoct the "recipe" for sand specimens of targeted D_r and most ideal homogeneity with a limited number of attempts.

Table 4.2: Attempts for Geba sand specimens $D_r = 40\%$

	Variables			D_r	Comments
	Falling Height	Opening Width	Box Speed		
Attempt 1	240 mm	1.0 mm	15 mm/s	52%	Too dense
Attempt 2	240 mm	1.5 mm	15 mm/s	49%	Too dense
Attempt 3	180 mm	1.5 mm	15 mm/s	39%	Good

Table 4.3: Attempts for Geba sand specimens $D_r = 80\%$

	Variables			D_r	Comments
	Falling Height	Opening Width	Box Speed		
Attempt 4	240 mm	1.3 mm	30 mm/s	57%	Too loose
Attempt 5	540 mm	1.3 mm	30 mm/s	77%	Basically good

4.4. Homogeneity Check for Pluviated Specimens

Lastly, the homogeneity of the Geba sand specimens was checked. As supposed, the "recipe" for the relative density of 80% (de facto 77%) should make the specimens relatively uniform, due to the small Opening Width. In contrast, the specimens of 40% (de facto 39%) relative density should be more obviously stratified.

To explore the uniformity of the Geba sand specimens, a special sample was prepared, whose lower half was prepared using the "recipe" for Attempt 5, and the upper half was prepared using the "recipe" for Attempt 3. The CT image is shown in Figure 4.2.
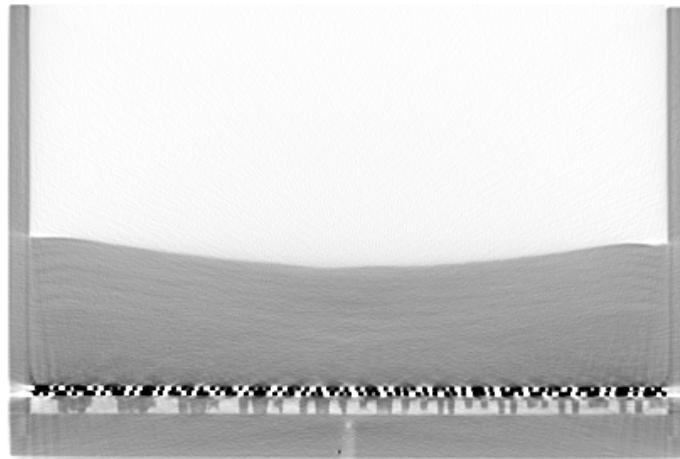
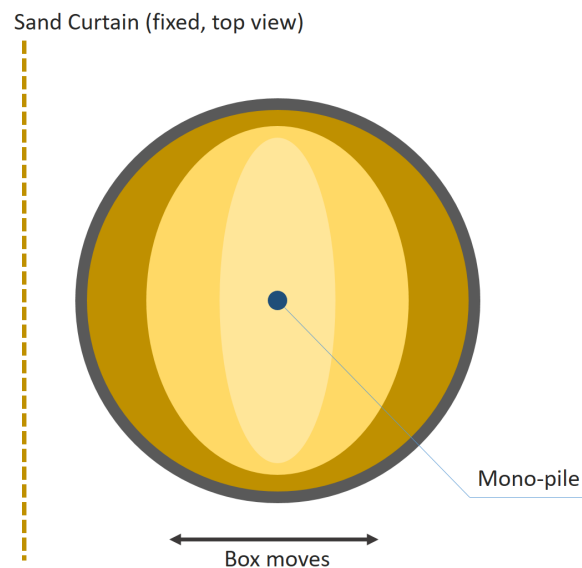Figure 4.2: The CT image of the Geba sand sample G01

Figure 4.3: The horizontal heterogeneity sketch of cylinder sand specimens

As can be seen, the upper half indeed has a more obvious feature of stratification, and the downer half is more uniform. Besides, as no sharp edges (as explained in Figure 3.5) was applied for this series of tests, the height of the pluviated sand body is smaller in the middle part and larger near the boundary.

What is more, the pluviated sand body is relatively denser near the boundary and looser in the middle. This phenomenon is obvious in the section perpendicular to the "sand curtain" but ignorable in the parallel sections, as shown in Figure 4.3, where darker yellow represents denser sand packing, vice versa. Therefore, for cylinder sample boxes, it is recommended to rotate the box horizontally during the process of pluviation. At least, the user of the sand pluviator should attach significance to the direction of horizontal loading (e.g. lateral loading for mono-pile), if applicable.

5

Conclusions

Firstly, it was proved by a series of repetitive tests that the line-style sand pluviator of TU Delft is capable of preparing sand samples of controllable bulk relative density. By controlling the execution parameters Falling Height, Opening Width and Box Speed, specimens with D_r ranging from 50% to 100% can be prepared, using the coarse Merwede River sand. Besides, the fullness of sand hopper, initial state of stored sand and the potential dynamic crushing and abrasion of sand particles are important as well, as these indexes may result in the unacceptable deviation of the relative density and make the sample preparation work unrepeatable, if are not properly controlled.

Furthermore, the general relationship among the bulk relative density and three variables were concluded. The relative density is positively correlated with Falling Height and negatively correlated with Opening Width, with some exceptions, although. The relationship between D_r and Box Speed is not monotonic. Based on the pluviation tests, CT scanning results and high frame rate photographs, a partially substantiated hypothesis of the three variables' influences on the relative density was proposed, and this hypothesis provides practical advices on preparing samples using the Geba sand.

Additionally, using the macro-CT scanner, it was observed that stratification is obvious in the specimens prepared by the pluviation method. The variation of local relative density along depth is analogous to a trigonometric function and the shape of the function is generally controllable by changing the values of three variables. Using the micro-CT scanner, it was observed that the inclination of sand particles and the grading conditions are distinct in different layers of the stratified specimens and one should attach importance to these phenomena, as the variation of local relative density and other fabric features of sand significantly affect the behaviour of specimens in different types of physical modelling tests, including the shallow foundation tests in which a difference of 38% for bearing capacity was found between two specimens with the same bulk relative density but different stratifying conditions. Apart from exploring the influences of the stratifying heterogeneity, it is also recommended to focus on the air-water pluviation method to make it possible to prepare loose and more homogeneous specimens.

Bibliography

[1] K. A. Alshibli, A. M. Druckrey, R. I. Al-Raoush, T. Weiskittel, and N. V. Lavrik. Quantifying morphology of sands using 3d imaging. *Journal of Materials in Civil Engineering*, 27(10):04014275, 2015. doi: 10.1061/(ASCE)MT.1943-5533.0001246.

[2] E. Andò, G. Viggiani, S. A. Hall, and J. Desrues. Experimental micro-mechanics of granular media studied by x-ray tomography: recent results and challenges. *Géotechnique Letters*, 3(3):142–146, 2013. doi: 10.1680/geolett.13.00036.

[3] K. Arulanandan. A directional structure index related to sand liquefaction. In *Proceedings of the ASCE Geotechnical Engineering Division Specialty Conference*, pages 213–230, 1978.

[4] A. Askarinejad. *Failure mechanisms in unsaturated silty sand slopes triggered by rainfall.* PhD thesis, ETH Zürich, 2013.

[5] P. J. Barrett. The shape of rock particles, a critical review. *Sedimentology*, 27(3):291–303, 1980. doi: 10.1111/j.1365-3091.1980.tb01179.x.

[6] J. Bolouri Bazaz, M. Zadehmohamad, and S. S. Hashemi. Developing a portable curtain sand pluviator for reconstitution of soil models (in persian). *Modares Civil Engineering journal*, 18(1), 2018.

[7] M. D. Bolton. The strength and dilatancy of sands. *Géotechnique*, 36(1):65–78, 1986. doi: 10.1680/geot.1986.36.1.65.

[8] E. T. Bowman and K. Soga. Creep, ageing and microstructural change in dense granular materials. *Soils and Foundations*, 43(4):107–117, 2003. doi: 10.3208/sandf.43.4_107.

[9] R. Butterfield and K. Z. Andrawes. An air activated sand spreader for forming uniform sand beds. *Géotechnique*, 20:97–100, 1970.

[10] S. C. Chian, M. E. Stringer, and S. P. G Madabhushi. Use of the automatic sand pourers for loose sand models. In *Proceedings of the 7th International Conference on Physical Modelling in Geotechnics, 7th ICPMG '10*, pages 117–121, 2010.

[11] S. Choi, M. Lee, H. Choo, M. T. Tumay, and W. Lee. Preparation of a large size granular specimen using a rainer system with a porous plate. *Geotechnical Testing Journal*, 33(1):45–54, 2010. doi: 10.1520/GTJ101634.

[12] G. Coriolis. Mémoire sur le principe des forces vives dans les mouvements relatifs des machines (in french). *Journal de l'École polytechnique*, 13(21):268–302, 1832.

[13] J.-F. Corté, Garnier J., L. M. Cottineau, and G. Rault. Determination of model soil properties in the centrifuge. In *Proceedings of the International Conference on Geotechincal Centrifuge Modelling*, 1991.

[14] A. Cresswell, M. Barton, and R. Brown. Determining the maximum density of sands by pluviation. *Geotechnical Testing Journal*, 22(4):324–328, 1999. doi: 10.1520/GTJ11245J.

[15] J. R. Curray. The analysis of two-dimensional orientation data. *The Journal of Geology*, 64(2):117–131, 1956. doi: 10.1086/626329.

[16] T. N. Dave and S. M. Dasaka. Assessment of portable traveling pluviator to prepare reconstituted sand specimens. *Geomechanics and Engineering*, 4(2):79–90, 2012.

[17] J. Desrues, R. Chambon, M. Mokni, and F. Mazerolle. Void ratio evolution inside shear bands in triaxial sand specimens studied by computed tomography. *Géotechnique*, 46(3):529–546, 1996. doi: 10.1680/geot.1996.46.3.529.

[18] C. Fretti, D. Lo Presti, and S. Pedroni. A pluvial deposition method to reconstitute well-graded sand specimens. *Geotechnical Testing Journal*, 18(2):292–298, 1995. doi: 10.1520/GTJ10330J.

[19] J. Garnier and L. M. Cottineau. La centrifugeuse du lcpc: moyens de préparation des modèles et instrumentation (in french). In *Proc. Centrifuge 88*, pages 83–90, 1988.

[20] K. G. Gavin and B. M. Lehane. The shaft capacity of pipe piles in sand. *Canadian Geotechnical Journal*, 40(1):36–45, 2003. doi: 10.1139/t02-093.

[21] M. G. Gomez, J. T. DeJong, and C. M. Anderson. Effect of bio-cementation on geophysical and cone penetration measurements in sands. *Canadian Geotechnical Journal*, 55(11):1632–1646, 2018. doi: 10.1139/cgj-2017-0253.

[22] M. Hakhamaneshi, J.A. Black, A. Cargill, C.M. Cox, and T. Elmrom. Development and calibration of a sand pluviation device for preparation of model sand bed for centrifuge tests. In *Proceedings of the 3rd European Conference on Physical Modelling in Geotechnics*, pages 73–79, 2016.

[23] C. Hariprasad, M. Rajashekhar, and B. Umashankar. Grain-scale characterization of water retention behaviour of sand using x-ray ct. *Geotechnical and Geological Engineering*, 34:1909–1922, 2016. doi: 10.1007/s10706-016-0064-0.

[24] M. A. Hicks and W. A. Spencer. Influence of heterogeneity on the reliability and failure of a long 3d slope. *Computers and Geotechnics*, 37(7):948–955, 2010. ISSN 0266-352X. doi: https://doi.org/10.1016/j.compgeo.2010.08.001.

[25] M.Z. Hossain and M.A. Ansary. Development of a portable traveling pluviator device and its performance to prepare uniform sand specimens. *Innovative Infrastructure Solutions*, 3(53), 2018. doi: 10.1007/s41062-018-0159-y.

[26] American Petroleum Institute. *Recommended practice for planning, designing and constructing fixed offshore platforms — Working stress design, 20th ed. API RP2A-WSD*. 1993.

[27] ISO. *ISO 9276-6:2008: Representation of results of particle size analysis – Part 6: Descriptive and quantitative representation of particle shape and morphology*. 2008.

[28] G. Khaddour, I. Riedel, E. Andò, P. Charrier, P. Bsuélle, J. Desrues, G. Viggiani, and S. Salager. Grain-scale characterization of water retention behaviour of sand using x-ray ct. *Acta Geotechnica*, 13:497–512, 2018. doi: 10.1007/s11440-018-0628-7.

[29] M. Khari, K. A. Kassim, and A. Adnan. Sand samples' preparation using mobile pluviator. *Arabian Journal for Science and Engineering*, 39:6825–6834, 2014. doi: 10.1007/s13369-014-1247-8.

[30] J. J. Kolbuszewski. An experimental study of the maximum and minimum porosities of sands. In *Proceedings of the Second International Conference of Soil Mechanics and Foundation Engineering*, volume 1, pages 158–165, 1948.

[31] J. J. Kolbuszewski and R. H. Jones. The preparation of sand samples for laboratory testing. In *Proceedings of the Midland Soil Mechanics Foundation Engineering Society*, volume 4, pages 107–123, 1961.

[32] C. Krapfenbauer. Experimental investigation of static liquefaction in submarine slopes. Master's thesis, ETH Zürich, 2016.

[33] R. Lagioia, A. Sanzeni, and F. Colleselli. Air, water and vacuum pluviation of sand specimens for the triaxial apparatus. *Soils and Foundations*, 46(1):61–67, 2006. doi: 10.3208/sandf.46.61.

[34] K. L. Lee. *Triaxial compressive strength of saturated sand under seismic loading conditions*. PhD thesis, University of California, Berkeley, 1965.

[35] D. C. F. Lo Presti, R. Berardi, S. Pedroni, and V. Crippa. A new traveling sand pluviator to reconstitute specimens of well-graded silty sands. *Geotechnical Testing Journal*, 16(1):18–26, 1993. doi: 10.1520/GTJ10263J.

[36] S. P. G. Madabhushi, N. E. Houghton, and S. K. Haigh. A new automatic sand pourer for model prepara-
      tion at university of cambridge. In *Proceedings of the 6th International Conference on Physical Modelling
      in Geotechnics*, volume 1, pages 217–222, 2006.

[37] A. Maghsoudloo, A. Askarinejad, R. R. de Jager, F. Molenkamp, and M. A. Hicks. Experimental investiga-
      tion of pore pressure and acceleration development in static liquefaction induced failures in submerged
      slopes. In *Proceedings of the 9th International Conference on Physical Modelling in Geotechnics*, pages
      987–992, 2018.

[38] D. Mancarella and V. Simeone. Capillary barrier effects in unsaturated layered soils, with special refer-
      ence to the pyroclastic veneer of the pizzo d'alvano, campania, italy. *Bulletin of Engineering Geology and
      the Environment*, 71:791–801, 2012. doi: 10.1007/s10064-012-0419-6.

[39] MathWorks. *MATLAB*. 2019.

[40] P. W. Mayne and H. G. Poulos. Approximate displacement influence factors for elastic shallow founda-
      tions. *Journal of Geotechnical and Geoenvironmental Engineering*, 125(6):453–460, 1999. doi: 10.1061/
      (ASCE)1090-0241(1999)125:6(453).

[41] J. K. Mitchell and K. Soga. *Fundamentals of soil behavior*. 3 edition, 2005.

[42] S. Miura and S. Toki. A sample preparation method and its effect on static and cyclic deformation-
      strength properties of sand. *Soils and Foundations*, 22(1):61–77, 1982. doi: 10.3208/sandf1972.22.61.

[43] M. Oda. Initial fabrics and their relations to mechanical properties of granular material. *Soils and Foun-
      dations*, 12(1):17–36, 1972. doi: 10.3208/sandf1960.12.17.

[44] M. Oda. The mechanism of fabric changes during compressional deformation of sand. *Soils and Foun-
      dations*, 12(2):1–18, 1972. doi: 10.3208/sandf1972.12.1.

[45] M. Oda and I Koishikawa. Strength anisotropy of sand ground and its significance in soil engineering (in
      japanese). In *Proceedings of the Japan Society of Civil Engineers*, volume 1978, pages 111–120, 1978. doi:
      10.2208/jscej1969.1978.273_111.

[46] S. T. O'Donnell, B. E. Rittmann, and E. Kavazanjian. Midp: Liquefaction mitigation via microbial deni-
      trification as a two-stage process. i: Desaturation. *Journal of Geotechnical and Geoenvironmental Engi-
      neering*, 143(12):04017094, 2017. doi: 10.1061/(ASCE)GT.1943-5606.0001818.

[47] M. C. Powers. A new roundness scale for sedimentary particles. *Journal of Sedimentary Research*, 23(2):
      117–119, 1953. doi: 10.1306/D4269567-2B26-11D7-8648000102C1865D.

[48] A. Rabbani, S. Ayatollahi, R. Kharrat, and N. Dashti. Estimation of 3-d pore network coordination num-
      ber of rocks from watershed segmentation of a single 2-d image. *Advances in Water Resources*, 94:264 –
      277, 2016. doi: https://doi.org/10.1016/j.advwatres.2016.05.020.

[49] R. Rorato, M. Arroyo, A. Gens, E. Andò, and G. Viggiani. Particle shape distribution effects on the triaxial
      response of sands: A dem study. In *Micro to MACRO Mathematical Modelling in Soil Mechanics*, pages
      277–286, 2018.

[50] A. N. Schofield. Cambridge geotechnical centrifuge operations. *Géotechnique*, 30(3):227–268, 1980. doi:
      10.1680/geot.1980.30.3.227.

[51] D. Seo, C. Sohn, M. B. Cil, and G. Buscarnera. Evolution of particle morphology and mode of fracture
      during the oedometric compression of sand. *Géotechnique*, 0(0):1–13, 2020. doi: 10.1680/jgeot.18.P.300.

[52] W. O. Smith, P. D. Foote, and P. F. Busang. Packing of homogeneous spheres. *Physical Review*, 34:1271–
      1274, 1929. doi: 10.1103/PhysRev.34.1271.

[53] Japanese Geotechnical Society. *The laboratory testing standards of geomaterials*. 2015.

[54] H. G. Stuit. *Sand in the geotechnical centrifuge*. PhD thesis, TU Delft, 1995.

[55] F. S. Tehrani, A. Askarinejad, and F. Schenkeveld. Preliminary results of laboratory analysis of sand fluidisation. In *Proceedings of the 9th International Conference on Physical Modelling in Geotechnics*, pages 461–464, 2018.

[56] Y.P. Vaid and D. Negussey. Relative density of pluviated sand samples. *Soils and Foundations*, 24(2): 101–105, 1984. doi: 10.3208/sandf1972.24.2_101.

[57] Y.P. Vaid and D. Negussey. Preparation of reconsituted sand specimens. *Advanced Triaxial Testing of Soil and Rock*, pages 405–417, 1988. doi: 10.1520/STP29090S.

[58] S. J. M. van Adrichem. Influence of rapid draw down on dike stability. Master's thesis, TU Delft, 2021.

[59] H. Wadell. Volume, shape, and roundness of rock particles. *The Journal of Geology*, 40(5):443–451, 1932. doi: 10.1086/623964.

[60] H. Wadell. Sphericity and roundness of rock particles. *The Journal of Geology*, 41(3):310–331, 1933. doi: 10.1086/624040.

[61] H. Wadell. Volume, shape, and roundness of quartz particles. *The Journal of Geology*, 43(3):250–280, 1935. doi: 10.1086/624298.

[62] D. Wijewickreme, S. Sriskandakumar, and P. Byrne. Cyclic loading response of loose air-pluviated fraser river sand for validation of numerical models simulating centrifuge tests. *Canadian Geotechnical Journal*, 42(2):550–561, 2005. doi: 10.1139/t04-119.

[63] J. A. Yamamuro and P. V. Lade. Static liquefaction of very loose sands. *Canadian Geotechnical Journal*, 34(6):905–917, 1997. doi: 10.1139/t97-057.

[64] J. A. Yamamuro and F. M. Wood. Effect of depositional method on the undrained behavior and microstructure of sand with silt. *Soil Dynamics and Earthquake Engineering*, 24(9):751 – 760, 2004. doi: 10.1016/j.soildyn.2004.06.004.

[65] J. Zheng and R. D. Hryciw. Traditional soil particle sphericity, roundness and surface roughness by computational geometry. *Géotechnique*, 65(6):494–506, 2015. doi: 10.1680/geot.14.P.192.